Tectonic controls on the spatial distribution and stratigraphic architecture of a net-transgressive shallow-marine syn-rift succession in a salt-influenced rift basin: Middle-to-Upper Jurassic, Norwegian Central North Sea

Abbreviated title:

Structural and stratigraphic architecture of a salt-influenced rift basin

ARUNA S. MANNIE*[1§], CHRISTOPHER A–L. JACKSON[1], GARY J. HAMPSON[1] & ALASTAIR J. FRASER[1]

[1]Basins Research Group (BRG), Department of Earth Science & Engineering, Imperial College, Prince Consort Road, London, SW7 2AZ, UK

[§]Present address: Premier Oil, 23 Lower Belgrave Street, London. SW1W 0NR

*E-mail of corresponding author: aruna.mannie@gmail.com

ABSTRACT

Syn-depositional deformation in salt-influenced rift basins is complex, being driven by a combination of normal faulting and the growth of salt structures such as diapirs. Due to a lack of data with which to simultaneously constrain basin structure and syn-rift stratigraphic architecture, we have a poor understanding of how these processes control shallow marine deposition in such settings. To improve our understanding we here use seismic reflection and borehole data from the Norwegian Central North Sea to investigate the role that syn-depositional fault growth and salt movement played in controlling the sub-regional stratigraphic architecture of a net-transgressive shallow-marine syn-rift succession (Middle-to-Late Jurassic). The rift-related structural framework, which is usually dominated by normal fault-bound horst and graben, is strongly modified where an Upper Permian salt layer (Zechstein Supergroup) is sufficiently thick and mobile to act as an intra-stratal detachment, giving rise to decoupled rift-related basement and cover structural styles. Furthermore, cover extension allows the salt to rise diapirically, resulting in the formation of large salt diapirs and supra-salt normal faults formed due to late-stage salt withdrawal and diapir collapse. Rift-related normal faulting and the growth of salt structures had a dual control on the depositional thickness and facies distribution within the net-transgressive, predominantly shallow-marine, Middle-to-Upper Jurassic syn-rift succession. The resulting facies architecture reflects a delicate balance between fault- and salt flow-driven accommodation creation and intra- and extra-basinal sediment supply. Where sediment supply and accumulation rate exceeded accommodation, little or no change in facies is observed across syn-depositional structures. In contrast, where accommodation outpaced sediment supply and accumulation rate, footwall-attached shorelines locally developed adjacent to large, thick-skinned normal faults, with deeper water conditions persisting in the adjacent hanging wall. Flooding of individual structural

elements was strongly diachronous and influenced by the underlying rift-related topography, which was characterised by intra-basinal horst and graben. This paper highlights the key role that salt plays in modifying the tectono-stratigraphic evolution of rift basins, suggesting that existing models, based on salt-free structural templates, need to be modified.

INTRODUCTION

Rift basins may contain pre-rift salt (e.g., Upper Triassic Keuper salt, northern Iberian margin of Iberia; Rowan, 2014), which may act as an intra-stratal detachment that decouples rift-related basement and cover deformation. For example, fault-related folding of the cover, in addition to salt-detached extension, is particularly common in salt-influenced rifts due to the decoupling effects of salt (e.g., Stewart *et al.* 1996; Stewart & Clark 1999; Corfield & Sharp 2000; Ford et al., 2007; Stewart 2007; Marsh *et al.* 2010; Duffy *et al.* 2013; Lewis *et al.* 2013; Wilson *et al.* 2013). In addition to representing an intrastratal detachment that simply facilitates cover folding and faulting, thin-skinned extension and basement tilting may themselves lead to flow of salt and the development of large reactive diapirs (e.g., Vendeville & Jackson 1992a; Stewart & Clark 1999; Dooley et al., 2005). The structural style of rifts containing salt may thus be characterised by fault- and salt-related structures and, therefore, these basins may be more complex (e.g., Alves *et al.* 2003; Stewart 2007; Jackson & Lewis, 2016) than those lacking salt, which are typically dominated by normal faults (e.g. Gawthorpe & Leeder, 2000).

Because the structural style and evolution of salt-influenced rifts is complex and ultimately controls rift physiography, and uplift and subsidence patterns, the way in which syn-rift sediment is sourced, dispersed and deposited is accordingly complex. For example, syn-depositional growth of salt structures may locally influence the thickness, stratigraphic

architecture and facies distribution within syn-rift strata, with strata commonly thinning from salt-bound depocentres towards salt-cored structural highs, which may occur in concert with a reduction in water depth and a shallowing of the representative marine facies (Davison *et al.* 1996; Alves *et al.* 2003; Aschoff & Giles 2005; Shelley & Lawton, 2005; Kieft *et al.* 2010; Mannie *et al.* 2014a). However, if sediment accumulation rate exceeds diapir rise rate, little at-surface relief may develop and no variations in water depth may occur; in this case, facies belts may be relatively confined, with syn-depositional subsidence merely leading to the preservation of thickened successions in the centre of flanking minibasins (Banham & Mountney 2013). Furthermore, extensional collapse of salt diapirs may result in the formation of supra-diapir minibasins that provide local accommodation for thick sedimentary successions that may, or may not, be associated with rapid lateral facies transitions (Wakefield *et al.* 1993; Stewart & Clark 1999; Hudec *et al.* 2009; Mannie *et al.* 2014b). The key challenge is that these purely halokinesis-driven depositional styles may be superimposed on prior and/or synchronously forming rift-related structural geometries, or they may be spatially partitioned in areas of the rift dominating by thick, mobile salt (e.g., Erratt 1993; Stewart 2007).

Our understanding of the regional, syn-rift tectono-stratigraphic evolution of salt-influenced rift basins, and the specific role that faulting and salt flow plays in controlling syn-rift stratigraphic architectures, is limited because most studies are relatively local, and focus solely on either purely salt- or fault-controlled settings in individual hydrocarbon fields or sub-basins (e.g., Clark *et al.* 1998; Alves *et al.* 2003; Jackson *et al.* 2005; Kieft *et al.* 2010). Even when more regional studies are undertaken, the sedimentology and stratigraphy of syn-rift deposits are insufficiently integrated with the syn-depositional structural framework (e.g., Johnson *et al.* 1986; Wakefield *et al.* 1993; Spathopoulos *et al.* 2000; Duffy *et al.* 2013). Because of these issues, there are a number of unanswered

101 questions; for example, how does the presence of salt influence the early syn-rift
102 stratigraphic architecture in rift basins? And to what extent can existing tectono-
103 stratigraphic models for rift basins, which are principally based on salt-free settings
104 (Gawthorpe & Leeder 2000), be applied to salt-influenced rift basins?

105 The aim of this study is to constrain the tectonic controls on early syn-rift, shallow
106 marine depositional patterns in a salt-influenced rift basin. In particular, we aim to identify
107 the various sub-, intra- and supra-salt structural styles and their influence on the deposition
108 of a net-transgressive, early syn-rift shallow-marine succession of early syn-rift age. We
109 focus on the eastern flank of the Norwegian Central North Sea Graben, which is an ideal
110 location to undertake this type of study because seismic reflection and borehole data are
111 relatively abundant, and a basinwide biostratigraphic framework allows us to link periods
112 of deformation and specific depositional styles between various structural domains. We
113 here focus on shallow marine syn-rift systems; the reader is referred to Banham and
114 Mountney (2013) for a detailed documentation of the response of fluvial systems to salt-
115 influenced rift basins (Triassic of the Central North Sea and Permo-Triassic of the
116 Precaspian Basin, Kazakhstan, and Lawton et al. (2001) and Poprawski et al. (2014) for a
117 detailed documentation of salt-influenced turbidite and carbonate deposition (Basque-
118 Cantabrian Basin, northern Spain).

119

120 **REGIONAL TECTONO-STRATIGRAPHIC FRAMEWORK**

121 The Viking Graben, the Central Graben and the Moray Firth Basin represent the three arms
122 of the trilete North Sea rift system (Fig. 1). During the Late Permian, the Central Graben
123 was located near the margin of a marine seaway (the North Permian Basin) that was
124 subject to high rates of evaporation. Several flooding-evaporation cycles resulted in

deposition of a thick, salt-bearing succession (Zechstein Supergroup) (Clark *et al.* 1998; Stewart & Clark 1999). Early Triassic rifting and cover extension triggered reactive diapirism of the Zechstein salt and the formation of large salt walls, which influenced the deposition of continental clastics of the Smith Bank and Skagerrak formations (McKie & Williams 2009) (Fig. 2). Uplift of the Mid-North Sea Dome during the Early Jurassic caused erosion of the uppermost Triassic succession, and resulted in the absence of Early-to-Middle Jurassic strata across much of the Central Graben due to non-deposition or post-depositional erosion (Mid-Cimmerian unconformity) (Underhill & Partington 1993). Thermal deflation and subsidence of the Mid North Sea Dome during the Middle Jurassic was synchronous with the initiation of rifting, and together these triggered marine flooding and prolonged (c. 30 Myr) retreat of shoreline systems southward along the axis of the northern and central North Sea and deposition of a net-transgressive shallow marine succession (Fig. 3; Rattey & Hayward 1993; Underhill & Partington, 1993; Andsbjerg *et al.* 2001). In the North Viking Graben, activity on rift-related faults initiated during the latest Bajocian-to-early Bathonian; further south, in the Moray Firth, faulting did not commence until the Bathonian-to-Callovian (e.g., Fraser *et al.* 2003; Husmo *et al.* 2003). Rifting and salt movement in the Central Graben led to complex temporal and spatial variations in the timing of flooding and diachronous deposition of the early syn-rift shallow marine succession within various parts of the graben (Fig. 3). For example, in the Norwegian sector of the Central Graben, flooding is recorded by the coastal-plain deposits of the Bryne Formation (Bajocian-Bathonian?), which are conformably overlain by shallow marine deposits of the Sandnes Formation (Callovian) in the Norwegian-Danish and Egersund basins (Fig. 2). In contrast, on the Cod Terrace, the Bryne Formation is unconformably overlain by shallow marine deposits of the Ula/Gyda Formation (Oxfordian-Kimmeridgian) (Fig. 2). Continued relative sea-level rise during the Late

Jurassic and Early Cretaceous, driven by rift-related and salt-influenced subsidence, led to an increase in water depth and deposition of shelfal and deep-marine deposits of the Tau, Sauda, Farsund, Mandal and Flekkefjord formations (Fig. 2). This study focuses on the impact that Middle-to-Upper-Jurassic, rift-related extension and salt tectonics had on the stratigraphic architecture of the early syn-rift Bryne, Sandnes and Ula/Gyda formations (J20- J70 units of Partington *et al.* 1993).

DATASET

To achieve our study aims, we use 2D and 3D seismic reflection data that cover a combined area of >15,000 km^2 on the eastern margin of the Central Graben, and data from 53 wells (Fig. 4). Seismic surveys S1-S4 were acquired between 1992 and 1999, and were reprocessed after 2000. These post-stack time-migrated datasets have a record length of 6000 milliseconds two-way time (ms TWT). The S5 dataset is a pre-stack time-migrated survey that was acquired in 2005 and has a record length of 6600 milliseconds two-way time (ms TWT). The 2D seismic survey was acquired in 1997 and is post-stack time-migrated. All wells fully penetrate the Middle-to-Upper-Jurassic succession and contain at least two conventional wireline logs (e.g., gamma ray, resistivity, density and sonic). These wells also contain checkshot data that allowed us to tie stratigraphic data (i.e. age and lithology) to the seismic reflection data. Twenty-six wells contain a total of 1180 m of core in the Middle-to-Upper-Jurassic succession. Biostratigraphic data were available for 21 wells, which allowed regional correlation between sub-basins and enabled us to tie our stratigraphic framework to the basinwide sequence stratigraphic framework of Partington *et al.* (1993).

METHODOLOGY

Four seismic horizons were mapped to define the regional structural framework of the study area (Fig. 2): (i) Top Rotliegend Group (c. 253.8 Ma), which defines the sub-salt, predominantly rift-related structure of the study area; (ii) Top Zechstein Supergroup (c. 251 Ma), which defines the present-day distribution and geometry of salt structures; (iii) Top Egersund Formation (c. 155.6 Ma), which lies within the Late Jurassic syn-rift succession; and (iv) Top Mandal Formation (c. 140 Ma), which broadly defines the top of the syn-rift succession and highlights the pattern of rift- and salt-related deformation in the supra-salt interval.

Biostratigraphic data allowed us to identify a number of age-constrained flooding surfaces (e.g., K10FS, J52FS, J32?FS) within the J20-J70 stratigraphic units that could be correlated to the North Sea-wide, sequence stratigraphic scheme of Partington *et al.* (1993) (Fig. 2). Checkshot data allowed these biostratigraphically defined flooding surfaces to be tied to seismic data through the construction of synthetic seismograms (e.g., Mannie *et al.* 2014a, b). Core data permitted sedimentological facies analysis of the Middle-to-Upper-Jurassic succession. Based on the vertical facies relationships observed in core, higher-order flooding surfaces were identified, such as those within the J40 unit (FS2 – FS4; Fig. 2). Wireline-log responses were calibrated to core descriptions in order to qualitatively interpret lithology and facies in uncored intervals. Flooding surfaces interpreted in core and wireline-log data were combined with seismic mapping and biostratigraphic data (calibrated to the scheme of Partington *et al.* 1993) in order to construct a sequence stratigraphic framework for the Middle-to-Upper-Jurassic succession.

REGIONAL STRUCTURAL AND STRATIGRAPHIC FRAMEWORK

In order to understand the temporal and spatial development of rift- and salt-flow-related structural styles, and their control on the Middle-to-Upper Jurassic (J20-J70) syn-rift stratigraphic development of the eastern Central Graben, sub-regional structure and time-thickness (isochron) maps were integrated with biostratigraphic data, sedimentological core descriptions and wireline-log analysis.

The three main structural elements within the study area are: (i) the platform areas of the Cod Terrace and Stavanger Platform; (ii) intra-basinal highs such as the Sørvestlandet High, Sele High and Lista Nose; and (iii) basinal areas of the Norwegian-Danish and Egersund basins (Fig. 4). The main structural styles include: (i) basement-involved normal faults, which may or may not breach the salt and which formed in response to Permo-Triassic and Jurassic-to-Early Cretaceous rifting; (ii) salt structures, which formed in response to flow of Zechstein salt; and (iii) supra-salt normal faults, which formed in response to a combination of flow of the Zechstein salt and stretching of the cover by Jurassic-to-Early-Cretaceous thick- and thin-skinned extension (Figs 5a and 6).

Sedimentological facies analysis of core from the Ula/Gyda Formation (J50-J70 unit) on the Cod Terrace, and the Bryne and Sandnes formations in the Egersund Basin (J20-J40) identified four main facies associations (Table 1): (i) offshore shelf: which comprises silty mudstone and a pinstriped siltstone dominated by *Anconichnus* and *Chrondrites* trace fossil assemblages; (ii) offshore transition: which comprises bioturbated and hummocky cross-stratified siltstone to very-fine grained sandstone in which *Teichichnus* and *Terebellina* trace fossil assemblages are common; (iii) shoreface: which comprises either a highly bioturbated, hummocky cross-stratified sandstone or a cross-stratified sandstone with planar lamination, symmetrical ripples and trough cross-bedding. Trace fossil assemblage in the shoreface are quite diverse, and are dominated by *Thalassinoides,*

Ophimorpha, Skolithos and *Teichichnus*; and (iv) coastal-plain: which is variable in character but which generally comprises rooted sandstones, coal, organic-rich mudstones, barren shales and cross-stratified sandstones. Organic-rich mudstones contain a low-diversity *Planolites* trace fossil assemblage (Table 1).

A regional SW-NE-oriented stratigraphic cross-section (from the Cod Terrace to the Stavanger Platform, Fig. 4) through the Middle-to-Upper-Jurassic early syn-rift succession suggests that the poorly dated coastal-plain deposits of the J20? unit (Aalenian-Bajocian) are present on the Cod Terrace and in the Norwegian-Danish and Egersund basins, but are absent on the Sørvestlandet High (Fig. 7). On the Cod Terrace these J20? (Aalenian-Bajocian) coastal-plain deposits are overlain by J50 (Oxfordian-Kimmeridgian) shallow-marine deposits, whereas to the east of the Sørvestlandet High, in the Egersund Basin, they are overlain by the older, J40 (Callovian-Oxfordian) coastal-plain to shallow-marine deposits. On the Sørvestlandet High, J70 (Portlandian-Ryazanian) offshore transition silty sandstones and marine shales directly overlie Triassic strata across the Mid-Cimmerian unconformity (Fig. 7).

We now describe the structural styles and stratigraphic succession present in the main geographical provinces using selected seismic cross-sections and isochron maps (Fig. 5), time-structure maps (Fig. 6), wireline-log and chronostratigraphic correlations (Figs 7, 8), and thickness and facies variations in the syn-rift succession (Table 2).

Cod Terrace

The structure and tectono-stratigraphic evolution of the Cod Terrace has been described in detail by Mannie et al. (2014b), thus only a brief overview of the key aspects pertinent to our sub-regional analysis is presented here. The Cod Terrace is a NW-trending, normal-

fault bounded terrace that is located on the eastern flank of the Central Graben (Fig. 4). Salt walls are common and they typically overlie sub-salt, basement-restricted, normal faults (Fig. 6b). Listric, salt-detached normal faults define the edges of salt walls and offset the upper part of the Triassic-Jurassic (Fig. 5a). Planar salt-detached normal faults are developed immediately above salt walls, offset Triassic-Jurassic strata, and define graben and half-graben containing thickened Upper Jurassic successions (Figs 5a and 6c).

On the Cod Terrace J20 (Aalenian-Bajocian) coastal-plain deposits represent the oldest penetrated Jurassic stratigraphic unit. These deposits are unconformably overlain by J50-J70 (Oxfordian-Ryazanian) shoreface sandstones and offshore mudstones; the unconformity separating these unit documents a hiatus of c.12 Myr (Fig. 7). Detailed seismic mapping of Upper Jurassic strata (J56-to-J71 FS; Oxfordian-Kimmeridgian) indicate that they were deposited in a series of minibasins formed in response to the extensional collapse of salt walls (Fig. 5b; Mannie *et al.* 2014b). An isochron map between the J66 and K10 flooding surfaces (Kimmeridgian-Ryazanian) also indicates abrupt thickening of Upper Jurassic strata across syn-depositional thin-skinned normal faults (Fig. 5d).

Sørvestlandet High

The NW-SE-trending horst of the Sørvestlandet High lies to the east of the Cod Terrace (Fig. 6). In contrast to the Cod Terrace, the Sørvestlandet High is defined by an array of sub-parallel, relatively elongate salt walls, which form a broadly polygonal network (see also Karlo et al., 2014). Salt stocks are locally developed along the salt walls, and are particularly common along the eastern margin of the Sørvestlandet High (Fig. 6b). In a similar way to the Cod Terrace, salt-detached listric and planar normal faults define the

edges of salt walls and offset the upper part of the Triassic-Jurassic, defining small graben and half-graben (Fig. 5a).

On the Sørvestlandet High, J70 (Portlandian-Ryazanian) offshore transition to offshore shelf deposits are the oldest preserved Jurassic strata and directly overlie the Triassic across the Mid-Cimmerian unconformity, which here represents a c. 60 Myr hiatus (Figs 2 and 7). Detailed seismic mapping of Upper Jurassic strata indicate that the J70 unit was deposited in a series of minibasins formed in response to the extensional collapse of salt walls, similar to that documented on the Cod Terrace (Fig. 5b). Well penetrations suggest that the J70 unit is less than 100 m thick on the Sørvestlandet High (Fig. 7).

Norwegian-Danish and Egersund basins

The Norwegian-Danish Basin is bounded to the west by the normal fault system that defines the eastern margin of the Sørvestlandet High, and to the east by the Egersund Basin (Figs 4 and 6a). In the Norwegian-Danish Basin, a mosaic of salt walls, which trend broadly NW-SE and are sub-parallel to the basement-involved normal fault systems, are present (Fig. 6b). Salt-detached normal faults in the Norwegian-Danish Basin are planar and offset Triassic-Jurassic strata, where they define small graben and half-graben (Fig. 5a).

To the northeast of the Norwegian-Danish Basin is the NW-SE-trending Egersund Basin, which is bounded to the NE, W and E by large displacement (up to 1.5 km) normal fault systems (Lewis *et al.* 2013; Mannie *et al.* 2014a) (Fig. 6a). In the Egersund Basin, the dominant salt structures are broadly NW-SE-trending salt walls that are situated above and trend parallel to basement-involved normal fault systems (Fig. 6b). Salt anticlines and salt rollers are also locally developed in the Egersund Basin (Fig. 6b), and salt-detached

297 normal faults are either listric and define the margins of salt rollers, or planar and bound
298 graben or half-graben developed above salt walls (Figs 5a, 5c and 6d).

299 In the Egersund Basin, J20 (Aalenian-Bajocian) coastal-plain deposits represent the
300 oldest preserved Jurassic strata, directly overlying Triassic strata across the Mid-
301 Cimmerian unconformity, which here represents a c. 30 Myr hiatus (Figs 7 and 8). J20
302 deposits in turn overlain by J40 unit (Callovian -Oxfordian) coastal-plain to shallow
303 marine deposits and J50-J70 units (Oxfordian-Ryazanian) offshore shelf mudstones (Figs 7
304 and 8). Well penetrations indicate that the Bryne and Sandnes formations (J20-J40 units)
305 thin towards the crest of several of the salt structures in the centre of the Egersund Basin
306 (Table 2; Mannie *et al.* 2014b). In the Egersund Basin, the J20-J70 units (Bajocian-
307 Portlandian) are laterally continuous unlike on the Cod Terrace and Sørvestlandet High
308 where they are restricted to supra-diapir depocentres (Figs 7b and 8).

309

310 **Timing of rifting and salt movement**

311 On the Cod Terrace and Sørvestlandet High, salt movement initiated in response to Early
312 Triassic rifting, resulting in reactive rise of salt and the formation of diapirs (Mannie *et al.*
313 2014b). Differential loading of the salt by non-marine clastic sediment drove subsequent
314 salt movement and passive diapir rise during the Late Triassic (Fig. 5a; Mannie *et al.*
315 2014b). Late Jurassic rifting reactivated the Permo-Triassic sub-salt normal faults, and
316 resulted in stretching of the overburden, widening and extensional collapse of pre-existing
317 diapirs, and formation of supra-salt normal faults and (supra-diapir) minibasins that
318 provided accommodation for deposition of the Middle-to-Upper Jurassic (J20-J70)
319 succession (Fig. 5b; Mannie *et al.* 2014b). Unlike on the Cod Terrace and Sørvestlandet
320 High, in which salt movement and diapir formation strongly influenced deposition during
321 the Triassic, salt movement in the Norwegian-Danish and Egersund basins occurred

predominantly in the Middle-to-Late Jurassic, being associated with the formation of reactive diapirs that influenced the thickness of the J20-J70 succession (compare Figs 5b and 5c; Mannie *et al.* 2014a, b).

TECTONO-STRATIGRAPHIC RECONSTRUCTIONS FOR THE NORWEGIAN CENTRAL NORTH SEA

In order to understand the impact of salt-influenced rifting on deposition of the net-transgressive, early syn-rift, Middle-to-Upper Jurassic shallow marine succession preserved in the Central North Sea, we constructed sub-regional tectono-stratigraphic maps using the seismic and borehole data described above. Facies distributions at the point of maximum regression below age-constrained flooding surfaces were combined with the Middle-to-Upper-Jurassic structural template derived from time-structure and isochron maps to construct maps for the following six time intervals; (i) Late Callovian (below FS2); (ii) Late Oxfordian (below J56FS); (iii) Early Kimmeridgian (below J62FS); (iv) Late Kimmeridgian (below J66AFS); (v) Portlandian (below J71FS); and (vi) Late Ryazanian (below K10FS) (Fig. 9).

Late Callovian (below FS2)

Below the FS2 flooding surface, shoreface and offshore shelf deposits of the Sandnes Formation (J40 unit) are present in the Norwegian-Danish and Egersund basins, with facies becoming progressively more distal from southeast to northwest (Figs 8 and 9a). A detailed NW-SE stratigraphic cross-section through the Egersund Basin illustrates marked diachroneity in the timing of deposition of the Sandnes Formation (Fig. 8), indicating that flooding to the east of the Sørvestlandet High occurred from the northwest during the

Callovian (Figs 8 and 9a). Although thickness changes attributable to Late Callovian, salt- and rift-driven differential subsidence are observed in J40 strata, a general lack of facies changes suggests that sediment supply and accumulation rate kept pace with the rate at which accommodation was generated, such that structural relief and water depth changes were relatively subdued (Figs 5c, 7 and Table 2; Mannie *et al.* 2014a). An exception to this occurs west of the Egersund Basin on the eastern flank of the Sele High, where a shoreface system was locally developed in the footwall of the Sele High Fault System; in the hangingwall of the fault, the age-equivalent interval is not only significantly thicker but also dominated by offshore mudstones, indicating that fault-driven subsidence rates were high enough to result in a marked change in accommodation, water depth and thus facies (Fig. 9a). The absence of the Sandnes Formation or its lateral age-equivalent on the Sørvestlandet High and Cod Terrace suggests these were topographic highs during the Callovian, and may have represented sediment sources that supplied sediment to the adjacent Norwegian-Danish and Egersund basins (Fig. 9a).

Late Oxfordian (below J56FS)

During the Late Oxfordian, the Norwegian-Danish and Egersund basins continued to deepen in response to ongoing extension rift-related normal faulting; this is recorded by deposition of the marine shales of the Egersund and Tau formations above the shallow marine Sandnes Formation (Figs 2 and 9b; Vollset & Doré, 1984). Late Oxfordian deposits are absent on the Sørvestlandet High and the northern part of the Cod Terrace, and Portlandian strata sit directly on the Sørvestlandet High (Figs 8 and 9b); these stratigraphic relationships suggest these structures were topographic highs during the Late Oxfordian (Fig. 9b). However, on the southern part of the Cod Terrace, Late Oxfordian shoreface

deposits of the Ula/Gyda Formation were locally preserved in supra-diapir minibasins that formed due to extensional diapir collapse as part of a connected network of valleys, with later differential erosion and preservation of strata playing only a minor role in the present-day thickness of these strata (Figs 5b and 9b; Mannie *et al.* 2014b).

Kimmeridgian (below J62FS and below J66AFS)

Rift-related subsidence and basin deepening continued into the Kimmeridgian in the Norwegian-Danish and Egersund basins, resulting in the deposition of anoxic shales of the Tau Formation (Fig. 2; Vollset & Doré 1984). In contrast, shallower water depths persisted on the northern part of the Cod Terrace with deeper offshore conditions to the south during the Early Kimmeridgian (below J62FS) (Fig. 9c). Increased accommodation above salt walls on the northern Cod Terrace during the Late Kimmeridgian (below J66AFS) resulted in shoreface deposition with offshore conditions persisting to the south (Fig. 9d). This increase in localised accommodation northwards on the Cod Terrace reflects the temporal and spatial variation in diapir collapse, which formed a linked network of valley-like depocentres, in contrast to the active basin-bounding faults in the Norwegian-Danish and Egersund basins that provided sub-regional subsidence in this rift margin location (Fig. 9c and d). On the Sørvestlandet High and the northernmost part of the Cod Terrace, Kimmeridgian deposits are absent, suggesting that, perhaps, these areas were topographic highs during the Callovian and represented sediment sources that supplied sediment to the adjacent Norwegian-Danish and Egersund basins (Fig. 9c and d).

Portlandian (below J72FS)

In the Norwegian-Danish and Egersund basins, marine shales of the Sauda Formation were deposited in the Portlandian due to continued high rates of subsidence and the persistence of deep-water condition in this rift margin location (Fig. 2; Vollset & Doré 1984). On the Sørvestlandet High, preservation of offshore transition deposits above salt walls reflects increased accommodation and/or increased preservation of these deposits above salt walls due to extensional diapir fall and transgression of this long-lived topographic high (Fig. 9e). To the west of the Sørvestlandet High on the Cod Terrace, preservation of offshore mudstones above salt walls suggests increased accommodation in this location, probably related to increased slip on the fault bounding the western margin of the Cod Terrace (Fig. 9e). We interpret that, at this time, the linked interconnected network of depocentres above salt walls on the Cod Terrace was connected to a similar network of supra-salt depocentres on the Sørvestlandet High (Fig. 9e).

Late Ryazanian (below K10FS)

In the Late Ryazanian, relatively deep-marine conditions had become established across the study area, resulting in the deposition of the marine shales of the Flekkefjord Formation in the Norwegian-Danish and Egersund basins, and the Mandal Formation on the Cod Terrace and Sørvestlandet High (Fig. 9f). Regional thermal subsidence, potentially coupled with a rise in eustatic sea-level, caused flooding of the Triassic highs and Jurassic minibasins on the Cod Terrace and Sørvestlandet High (Fig. 9f; Mannie *et al.* 2014b), with increased rates of fault-related extension in the Norwegian-Danish and Egersund basins (Lewis *et al.* 2013). This resulted in the landward migration (backstepping) of sand-rich

shorelines towards the basin margins and widespread deposition of offshore mudstones (Fig. 9f).

The Middle-to-Upper Jurassic sequence stratigraphic framework established by Partington *et al.* (1993) has been utilised by many workers in the central and northern North Sea, thereby enabling the work undertaken in this study to be compared to and integrated with, the results of previous regional studies (e.g., Fraser *et al.*, 2003 and Husmo *et al.*, 2003). The results of our high-resolution, chronostratigraphy-based approach, which integrates detailed structural mapping and stratigraphic analysis, challenge the notion that early syn-rift shallow marine sandstones occur in regionally continuous facies belts, an interpretation that was derived from a relatively low-resolution, lithostratigraphy-based, regional approach. Our palaeogeographic maps thus differ to those presented by Fraser *et al.* (2003) and Husmo *et al.* (2003), in that we explicitly account for complex temporal and spatial variation of marine incursion that resulted from the influence of underlying rift- and salt-related structures.

DISCUSSION

Tectono-sedimentary evolution of salt-influenced rift basins

The tectono-stratigraphic evolution of rift basins lacking salt has been documented in numerous studies (e.g., Leeder & Gawthorpe, 1987; Gabrielsen *et al.* 1990; Prosser 1993; Nøttvedt *et al.* 1995; Ravnås & Steel, 1998; Cowie *et al.* 2000) and is captured in widely cited conceptual models (Gawthorpe & Leeder 2000). These models predict that, during the initial stages of rifting ('rift initiation'; *sensu* Prosser 1993), abundant small normal faults and growth folds are developed, bounding numerous isolated depocentres (Gawthorpe & Leeder 2000). At this time, subsidence rates are relatively low, and

sediment accumulation rates may equal or exceed the rate at which accommodation is generated, thus leading to filled or overfilled basin conditions. Early syn-rift depocentres display marked variability in sedimentary fill, with sediment routing influenced by evolving fault- and fold-related patterns of differential subsidence and surface relief (Leeder & Gawthorpe 1987; Ravnås & Steel 1998; Gawthorpe & Leeder 2000). Shallow platforms that develop along the axis of the rift may become sites for shallow-marine sedimentation where they are connected to an external seaway (Mellere & Steel 1996; Ravnås & Steel 1998). As rifting continues, faults grow, interact and link, and tectonic subsidence becomes focussed within a small number of large, deep, interconnected depocentres. Fault slip rates and the rate of tectonic subsidence typically increase during the so-called 'rift climax' (*sensu* Prosser 1993), accelerating the rate of sea-level rise and marine transgression. The rift climax phase is typically characterised by a few large, through-going normal fault systems characterised by high displacement rates, such that tectonic subsidence outpaces sediment supply and accumulation rates in hanging wall depocentres, leading to widespread transgression at depocentre margins and sediment starvation in the basin axis if major intra-basin sediment sources are absent (Gawthorpe & Leeder 2000).

The presence of salt in the pre- or early syn-rift structural template of (salt-influenced) rift basins adds to the complexity of tectono-stratigraphic evolution implied by conceptual models lacking salt (compare Fig. 10a and 10b). For example, the growth and decay of salt diapirs can impact the stratigraphic thickness and facies distribution of syn-kinematic strata in two key ways. First, syn-tectonic strata typically become thinner and contain increasingly more proximal and/or shallower-water facies with increasing proximity to rising diapirs and salt-cored structural highs, (Davison *et al.* 1996; Alves *et al.* 2003; Kieft *et al.* 2010; Table 2). Second, diapir collapse due to ongoing extension may result in the

formation of fault-bound crestal minibasins (supra-diapir minibasins of Mannie et al., 2014b) that provide local accommodation (Wakefield *et al.* 1993; Stewart & Clark 1999; Mannie *et al.* 2014b; Fig. 5b and Table 2). Unlike rift basins that lack salt, within which accommodation and sediment routing is controlled by through-going, basement-involved normal faults and associated folds, the controls in salt-influenced rift basins are more complex, with sub-salt and supra-salt faults, and salt diapirs all playing a role (Fig. 10b). We now discuss the influence that these structures have on stratigraphic thickness and facies distributions during the deposition of the net-transgressive, shallow marine, Middle-to-Upper Jurassic early syn-rift succession studied here. We also broaden the results of our study to provide a general discussion of the tectono-stratigraphic evolution of salt-influenced basins located outside of the North Sea

Salt structures

In the Egersund Basin, extension resulted in the growth of salt structures such as salt anticlines and salt walls, which influenced the depositional thickness of the Middle-to-Upper Jurassic, coastal-plain to shallow-marine, early syn-rift succession (Fig. 10b). This is illustrated by well data, which indicate a reduction in thickness of this unit from the flank to the crest of the Xi salt anticline (25%) and the Alpha salt wall (45%) (Fig. 6b and Table 2; Mannie *et al.* 2014a). However, these thickness changes were not accompanied by a change in facies, suggesting that sediment accumulation rate outpaced the rate of accommodation creation across growing salt structures, and that minimal surface relief developed (Figs. 9 and 10; Mannie *et al.* 2014a). We suggest that high sediment accumulation rates, at least relative to diapir growth rate, was a function of the proximity of the Egersund Basin to the Norwegian mainland during the Jurassic, which would have

489 represented a major extra-basinal sediment source. However, in other salt-influenced rifts,
490 such as the Bombarral-Alcobaca sub-basin in Western Iberia, the rate of accommodation
491 generation outpaced sediment supply and accumulation, such that stratigraphic thinning of
492 21-42% of the syn-tectonic succession towards salt pillows, although comparable to that
493 observed in the Egersund Basin (25-45%), is accompanied by major facies change from
494 shallow-marine carbonates restricted to the pillow crests, to mudstone-dominated,
495 turbidite-bearing successions developed on the pillow flanks and adjacent minibasins
496 (Alves *et al.* 2003). Such a relationship between accommodation and sediment supply,
497 and the resultant thickness and facies changes, are not restricted to these salt-influenced
498 rift basins, but have also been described at outcrop from other tectonically active salt-
499 influenced settings, such as the Bakio salt diapir, northern Spain (Popwarski *et al*. 2014)
500 and the El Gordo diapir, NE Mexico (Giles *et al.* 2008). In both these areas, salt diapirs
501 form intra-basin relief flanked by shallower water depths and, therefore proximal facies
502 belts.

503 After initial reactive and possibly passive rise, exhaustion of autochthonous salt coupled
504 with ongoing extension can result in the collapse of diapirs and formation of supra-diapir
505 minibasins (e.g., Masson 1972; Mannie *et al.* 2014b; Fig. 10b). On the Cod Terrace,
506 formation of such minibasins during Late Jurassic regional extension resulted in the local
507 deposition and preservation of up to 500 m of coastal-plain to shallow-marine strata. In
508 comparison, fault-related subsidence in the Egersund Basin was responsible for
509 development of a laterally continuous net-transgressive succession up to 150 m thick
510 (Mannie *et al.* 2014a). As is typical of minibasins, these successions on the Cod Terrace
511 are thickest in the axis of the basin and thin (by up to 65%) towards the basin margins,
512 where they may be associated with a proximal to distal facies change from the flanks to the
513 axis of the minibasin (Fig. 5d and Table 2; Mannie *et al.* 2014b).

514

515 *Sub-salt normal faults*

516 Basement-involved, through-going normal faults that breach the salt and deform sub- and
517 supra-salt stratigraphy are observed on the eastern margin of the Sele High where salt is
518 thin and, potentially, rich in non-halite lithologies (e.g., anhydrite, carbonate) (Jackson and
519 Lewis, 2013). Formation of a large displacement, basement-involved normal fault resulted
520 in major footwall uplift and rotation, and deposition of a hanging wall shoreline that
521 developed downdip to the west of and that fringed, the Sele High (Figs 6a and 9a and
522 illustrated by the intra-basinal high in Fig. 10b; Mannie *et al.* 2014a). In the hanging-wall
523 of this fault, deeper-water conditions existed (Fig. 10b). The tectono-stratigraphic setting
524 of the Sele High thus conforms to the predictions of tectono-stratigraphic models
525 developed for salt-free rifts, with a strongly fault-controlled structural style resulting in
526 abrupt, across-fault changes in thickness and facies (Gawthorpe & Leeder 2000).

527 Active basement-involved, through-going normal faults can also influence sub-regional
528 subsidence and the timing of transgression as observed on the westerly bounding fault of
529 the Sørvestlandet High (Fig. 9e and f). Increased accommodation in this location, probably
530 related to increased rates of slip on the westerly bounding fault of the Cod Terrace at this
531 time, linked the interconnected network of supra-diapir minibasins developed on the Cod
532 Terrace to a similar network of minibasins on the Sørvestlandet High (Fig. 9e).

533

534

535 *Supra-salt normal faults*

Salt-detached normal faults can form relatively early in the salt-related basin history, accommodating cover extension and causing the growth of salt walls (e.g., Cod Terrace); in other circumstances, these faults may form relatively late in the basin history in response to extensional collapse of salt structures (Figs 5a, 5b and 10). Early faults related to rising diapirs clearly controlled bulk thickness changes in the Middle-to-Upper Jurassic succession, especially in the Egersund Basin (e.g., Figs 5e). The lack of well penetrations in graben that are bound by these faults means that we are unable to document whether these thickness changes are also associated with facies changes; however, based on well penetrations adjacent to salt-cored structural highs (see above), we consider that such changes are unlikely (Fig. 9a). This interpretation again suggests that high sediment supply and accumulation rates, which are directly linked to the basin-margin setting of the Egersund Basin, suppressed the development of significant intra-basin relief and water depth variations, and associated facies distributions, in the syn-rift succession (Fig. 9a).

Comparisons between salt-and non-salt influenced basins

Although we have focused on shallow-marine salt-influenced rifts, we extend our comparison to rifts lacking salt and those in other tectonic settings and depositional environments. In this way, we can further highlight the key role that intra-basin salt tectonics can have on basin physiography, accommodation development and the resultant stratigraphic architecture.

Comparisons between the salt-influenced Norwegian Central North Sea and non-salt influenced rift areas of the North Sea such as the East Shetland Basin and the Oseberg-Brage area located on the Horda Platform (Fig. 1), highlight the presence of a ductile evaporite layer in decoupling the sub- and supra-salt normal fault systems. In these

560 evaporite-free areas the structural styles are dominated by hard-linked normal fault relay
561 systems and growth-fault monoclines, where the underlying rift topography controls
562 accommodation, sediment distribution pathways and depositional processes. The
563 underlying structural topography of the Tern-Eider Horst, the Ninian-Hutton-Dunlin and
564 the North Alwyn-Brent-Statfjord fault systems in the East Shetland Basin and of the
565 Oseberg Fault in the Horda Platform area influenced the sediment dispersal and feeder
566 systems along the hanging-wall of normal faults during the deposition of the syn-rift,
567 shallow-marine, Middle Jurassic Tarbert Formation. As a result, the Tarbert Formation
568 thickness is variable, thinning towards footwall crests and thickening towards the hanging
569 wall of normal faults (Færseth & Ravnås 1998) with enhanced erosion and non-deposition
570 above growth fold monoclines prior to normal faults breaching the surface (Davies *et al.*
571 2000; Hampson *et al.* 2004). While activity along fault systems resulted in thickness
572 variations it did not result in major facies reorganisation due to a change in the balance
573 between sediment supply and subsidence (e.g., McLeod *et al.* 2002). Structurally-
574 controlled localised depocentres on the hanging wall of normal faults were a focus for
575 aggradational stacking of channel systems and shoreface successions, and led to strong
576 tidal influence where structurally controlled depocentres formed embayments or estuaries
577 with limited wave fetch (Hampson *et al.* 2004), particularly during transgression (Ravnås
578 *et al.* 1997). Similar thickness variations without major facies changes are observed in the
579 Egersund Basin within the study area (Table 2). Structurally controlled localised
580 depocentres on the hanging wall of normal faults (e.g., Egersund Basin) and within salt-
581 collapsed structures (e.g., Cod Terrace) contain aggradational wave-dominated shoreface
582 successions, rather than localised embayments with strong tidal influence. During the rift
583 climax phase, the Oseberg fault block in the Horda Platform area was subaerially exposed

584 in up-dip areas and eroded material from the footwall crest and deposited turbidites and
585 debris flow deposits in the hanging walls (Færseth & Ravnås 1998).

586 We here draw on outcrop examples from outside the North Sea to further highlight the
587 key role that salt diapirism has on accommodation development and stratigraphic
588 architecture. The Bakio salt diapir in the Basque-Cantabrian Basin, northern Spain is
589 interpreted as a reactive diapir initially formed in response to the Middle Albian movement
590 of the Gaztelugatxe normal fault, but which then grew passively during Middle to Late
591 Albian times (Popwarski *et al*. 2014). As it grew passively, the diapir formed an intra-
592 basin bathymetric high and was capped by a carbonate platform growing in relatively
593 shallow water. Syn-kinematic, middle to upper Albian turbidites were deposited in the
594 flanking minibasin, thinning and pinching-out towards the diapir crest (Popwarski *et al*.
595 2014). Unlike the Bakio diapir, the El Gordo diapir (Albian), which is located in the La
596 Popa Basin, Mexico, was a passive diapir formed in relatively shallow water depths in a
597 foreland basin. In a similar way to the Bakio diapir, shallowing of facies and stratal
598 thinning are recorded towards the diapir crest (Ashcoff & Giles 2005). In the Paradox
599 Basin, western US, salt movement initiated by differential loading of Carboniferous salt by
600 continental fluvial clastics of the Cutler Group (Banham & Mountney 2013). Here, salt-
601 walls are located above basement-involved normal faults and are flanked by deep
602 minibasins, in a structural configuration broadly similar to that described from the
603 Norwegian sector of the North Sea (Figure 6b). In this non-marine depositional
604 environment, sand-rich depositional systems, such as fluvial and aeolian systems, were
605 largely concentrated in the axis of minibasins. Above flanking salt walls, limited
606 accommodation resulted in sediment bypass, reworking and erosion by fluvial systems, or
607 the development paleosols in areas of especially low sediment accumulation rate (Banham
608 & Mountney 2013). Based on the examples presented above, we conclude that,

609 irrespective of the processes driving their growth, the key stratigraphic motif of syn-
610 depositional salt diapirism is overall thinning of strata towards the diapir crest, which may
611 be typically associated with intra-formational facies changes.

612 However, we argue there is key difference between overfilled, non-marine basins, such
613 as those typified by the Paradox Formation, and underfilled, marine basins, such as those
614 characterised by the Jurassic of the North Sea, the Bombarral-Alcobaca sub-basin, and the
615 Basque-Cantabrian and La Popa basins. In overfilled basins, facies partitioning might not
616 be as closely related to salt-driven changes in accommodation because, when overfilled,
617 the basin-floor would be flat, thus fluvial systems may be able avulse and deposit sheets of
618 sand across much of the basin width. In contrast, in underfilled marine basins, coarser-
619 grained shallow-marine systems are effectively 'pinned' to areas of low accommodation,
620 typically defined by salt diapirs. Deep marine systems may, of course, be deposited in
621 deep-water in flanking minibasins.

622

623 **CONCLUSIONS**

624 We used an integrated dataset of seismic and borehole data in order to reconstruct the
625 Middle-to-Upper Jurassic tectono-stratigraphic evolution of the Norwegian sector of the
626 Central North Sea. Our findings illustrate that the presence of salt in rift basins influences
627 structural style and stratigraphic architecture, which implies that established tectono-
628 stratigraphic models for rift basins cannot be applied where such basins contain mobile
629 salt. Key results are summarised below.

630 1. Unlike rift basins where salt is absent and the structural style is dominated by
631 growth folds and normal faulting, the presence of salt in a rift basin acts as a
632 detachment between the sub- and supra-salt cover structure. The resulting

structural styles can be defined by sub-salt normal faults, salt structures (e.g., salt walls, salt diapirs, salt rollers and salt anticlines) and supra-salt normal faults.

2. Extensional normal faulting and the growth of salt structures during syn-rift times influence depositional thickness and facies distributions. Stratigraphic thickness reduces from the flank to the crest of salt structures. Facies distributions are a function of accommodation creation and sediment supply. Where sediment supply equals or exceeds accommodation creation, no change in facies is observed during the growth of structures (e.g., Egersund Basin). In contrast, where creation of accommodation outpaces sediment supply localised shorelines are developed on the footwall of normal faults with deeper water conditions in the hanging wall (e.g., easterly bounding fault of the Sele High). Similar to rifts that lack salt, the timing of flooding is diachronous and localised topographic highs can result in the temporal and spatial variation of marine incursion.
3. The results presented in this paper highlight the distinct depositional evolutions of rift basins in the presence and absence of salt. During syn-rift times, depositional facies distributions vary in relation to subsidence rates, sediment supply and basin physiography.

ACKNOWLEDGEMENTS

The authors express their gratitude to the Norwegian Petroleum Directorate and PGS for providing access to seismic data. Centrica Energi Norge and the Commonwealth Commission are gratefully acknowledged for funding and support for this study, and Schlumberger Limited for use of Petrel software via an academic software donation. We

extend our gratitude to Mike Charnock for biostratigraphic analysis and related discussions. Adrian Hartley is acknowledged for his critical review and discussion of material in this manuscript. Roy Gabrielsen, Katherine Giles, an anonymous reviewer and Stephen Lokier are thanked for their critical reviews and editorial comments.

REFERENCES

ALVES, T. M., MANUPPELLA, G., GAWTHORPE, R. L., HUNT, D. W. & MONTEIRO, J. H. 2003. The depositional evolution of diapir- and fault-bounded rift basins: examples from the Lusitanian Basin of West Iberia. *Sedimentary Geology*, **162**, 273–303.

ANDSBJERG, J., NIELSEN, L. H., JOHANNESSEN, P. N. & DYBKJÆR, K. 2001. Divergent development of two neighbouring basins following the Jurassic North Sea doming event: the Danish Central Graben and the Norwegian-Danish Basin. In: MARTINSEN, O. J. & DREYER, T. (eds.) *Sedimentary Environments Offshore Norway - Palaeozoic to Recent.* Elsevier Science B.V., Amsterdam, Special Publication, **10**, 175-197.

ASCHOFF, J. L. & GILES, K. A. 2005. Salt diapir-influenced, shallow-marine sediment dispersal patterns: insights from outcrop analogs. *American Association of Petroleum Geologist*, Bulletin **89**, 447–469.

BANHAM S.G. & MOUNTNEY, N.P. 2013. Evolution of fluvial systems in salt-walled minibasins: A review and new insights. *Sedimentary Geology,* **296**, 142-166.

682 CLARK, J. A., STEWART, S. A. & CARTWRIGHT, J. A. 1998. Evolution of the NW
683 margin of the North Permian Basin, UK North Sea. *Journal of the Geological Society*,
684 *London,* **155**, 663-676.
685
686 CORFIELD, S. & SHARP, I. R. 2000. Structural style and stratigraphic architecture of
687 fault propagation folding in extensional settings: a seismic example from the Smørbukk
688 area, Halten Terrace, Mid-Norway. *Basin Research*, **12**, 329-341.
689
690 COWIE, P. A., GUPTA, S. & DAWERS, N. H. 2000. Implications of fault array evolution
691 for synrift depocentre development: insights from a numerical fault growth model. *Basin*
692 *Research*, **12**, 241-261.
693
694 DAVIES, S. J., DAWERS, N. H., MCLEOD, A. E. & UNDERHILL, J. R. 2000. The
695 structural and sedimentological evolution of early syn-rift successions: the Middle Jurassic
696 Tarbert Formation, North Sea. *Basin Research*, **12,** 343–365.
697
698 DAVISON, I., BOSENGE, D., ALSOP, G. I. & MOHAMMED, H. A.-A. 1996.
699 Deformation and sedimentation around active Miocene salt diapirs on the Tihama,
700 northwest Yemen. In: ALSOP, G. I., Blundell, D.J. & DAVISON, I. (eds.) *Salt Tectonics.*
701 *Geological Society London*, Special Publication, **100**, 23-39.
702
703 DOOLEY, T., MCCLAY, K.R., HEMPTON, M., SMIT, D., 2005. Salt tectonics above
704 complex basement extensional fault systems: results from analogue modelling. In: DORE'
705 A.G., & VINING, B.A.. (eds.) Petroleum Geology: north-west Europe a 6th Petroleum
706 Geology Conference: Geological Society London, 1631-1648.

DUFFY, O., GAWTHORPE, R.L., DOCHERTY, M. & BROCKLEHURST, S. H. 2013. Mobile evaporite controls on the structural style and evolution of rift basins: Danish Central Graben, North Sea. *Basin Research,* **25**, 310-330.

ERRATT, D. 1993. Relationships between basement faulting, salt withdrawal and Late Jurassic rifting, UK Central North Sea. In: PARKER, J. R. (ed.) *Petroleum Geology of Northwest Europe: Proceedings of the 4th Conference*. The Geological Society of London, 1211-1219.

FÆRSETH, R. B. & RAVNÅS, R. 1998. Evolution of the Oseberg fault-block in context of the northern North Sea structural framework. *Marine and Petroleum Geology,* **15**, 467-490.

FORD, M., LE CARLIER DE VESLUND, C., BOURGEOIS, ., 2007. Kinematic and geometric analysis of fault-related folds in a rift setting: the Dannemarie basin, Uppe Rhine Graben, France. *Journal of Structural Geology,* **29**, 1811-1830.

FRASER, S. I., ROBINSON, A. M., JOHNSON, H. D., UNDERHILL, J. R., KADOLSKY, D. G. A., CONNELL, R., JOHANNESSEN, P. & RAVNÅS, R. 2003. Upper Jurassic. In: EVANS, D., GRAHAM, C., ARMOUR, A., BATHURST, P. (eds.) *The Millennium Atlas: Petroleum Geology of the Central and Northern North Sea*. The Geological Society, London, 157–189.

GABRIELSEN, R. H., FÆRSETH, R.B., STEEL, R. J., IDIL, S. & KLØVJAN, O. S. 1990. Architectural styles of basin fill in the northern Viking Graben. In: BLUNDELL, D.

J. & GIBBS, A. D. (eds.) *Tectonic Evolution of the North Sea Rifts*. Clarendon, Oxford, 158-179.

GAWTHORPE, R. L. & LEEDER, M. R. 2000. Tectono-sedimentary evolution of active extensional basins. *Basin Research*, **12**, 195–218.

GILES, K.A., DRUKE, D.C., MERCER, D.W., & HUNNICUTT-MACK, L. 2008. Controls on Upper Cretaceous (Maastrichtian) heterozoan carbonate platforms developed on salt diapirs, La Popa basin, NE Mexico. SEPM publication **89**, 107–124.

HAMPSON, G. J., SIXSMITH, P. J., KIEFT, R. L., JACKSON, C. A-L., JOHNSON, H. D. 2009. Quantitative analysis pf net-transgressive shoreline trajectories and stratigraphic architectures:mid-tolate Jurassic of the North Sea rift basin. *Basin Research*, **21**, 528–558.

HAMPSON, G. J., SIXSMITH, P. J. & JOHNSON, H. D. 2004. A sedimentological approach to refining reservoir architecture in a mature hydrocarbon province: the Brent Province, UK North Sea. *Marine and Petroleum Geology,* **21**, 457–484.

HUSMO, T., HAMAR, G. P., HOILAND, O., JOHANNESSEN, E. P., ROMULD, A., SPENCER, A. M. & TITTERTON, R. 2003. Lower and Middle Jurassic. In: EVANS, D., GRAHAM, C., ARMOUR, A., BATHURST, P. (eds.) *The Millennium Atlas: Petroleum Geology of the Central and Northern North Sea*. The Geological Society, London, 129–156.

HUDEC, M. R., JACKSON, M. P. A., SCHULTZ-ELA, D. D. 2009. The paradox of minibasin subsidence into salt: Clues to the evolution of crustal basins. *Geological Society of American Bulletin*, **121**, 201–221.

JACKSON, C. A.-L. & LEWIS, M.M. 2016. Structural style and evolution of a salt-influenced rift basin margin: the impact of variations in salt composition and the role of polyphase extension. *Basin Research*, **28**, 81–102.

JACKSON, C. A.-L., GAWTHORPE, R. L. & SHARP, I. R. 2005. Normal faulting as a control on the stratigraphic development of shallow marine syn-rift sequences: the Nukhul and lower Rudeis Formations, Hammam Faraun fault block, Suez Rift, Egypt. *Sedimentology*, **52**, 313–338.

JACKSON C. A.-L., LEWIS M.M. 2013. Physiography of the North Permian Basin margin: new insights from 3D seismic reflection data. *Journal of the Geological Society*, **170**, 857-860.

JOHNSON, H. D., MACKAY, T. A. & STEWART, D. J. 1986. The Fulmar Oil-field (Central North Sea): geological aspects of its discovery, appraisal and development. *Marine and Petroleum Geology*, **3**, 99-125.

KARLO, J.F., VAN BUCHEM, FRANS S.P., MOEN, J. & MILROY, K. 2014. Triassic-age salt tectonic of the Central North Sea. *Interpretation*, **4**,19-28.

KIEFT, R. L., JACKSON, C. A.-L., HAMPSON, G. J. & LARSEN, E. 2010. Sedimentology and sequence stratigraphy of the Hugin Formation, Quadrant 15, Norwegian sector, South Viking Graben. In: VINING, B. A. & PICKERING, S. C. (eds.) *Petroleum Geology: From Mature Basins to New Frontiers – Proceedings of the 7th Petroleum Geology Conference*. The Geological Society of London, 157-176.

LAWTON, T.F., VEGA, F.J., & ROSALES-DOMINGUES, C. 2001. Stratigraphy and origin of the La Popa basin, Nuevo Leon and Coahuila, Mexico. In: BARTOLINI, C., BUFFLER, R.T. & CANTU`-CHAPA, A. (eds.) Mesozoic and Cenozoic evolution of the western Gulf of Mexico basin: Tectonics, sedimentary basins and petroleum systems. *American Association of Petroleum Geologist,* Memoir **75**, 219-240.

LEEDER, M. R. & GAWTHORPE, R. L. 1987. Sedimentary models for extensional tilt-block/half-graben basins. *Geological Society, London*, Special Publications, **28**, 139-152.

LEWIS, M. M., JACKSON, C. A.-L. & GAWTHORPE, R. L. 2013. Salt-influenced normal fault growth and forced folding: The Stavanger Fault System, North Sea. *Journal of Structural Geology*, **54**, 156-173.

MANNIE, A. S., JACKSON, C. A.-L & HAMPSON, G. J. 2014a. Structural controls on the stratigraphic architecture of net-transgressive shallow-marine strata in a salt-influenced rift basin: Middle-to-Upper Jurassic Egersund Basin, Norwegian North Sea. *Basin Research,* **26**, 675-700.

MANNIE, A. S., JACKSON, C. A.-L. & HAMPSON, G. J. 2014b. Shallow marine reservoir development in extensional diapir collapse minibasins: an integrated subsurface case study from the Upper Jurassic of the Cod Terrace, Norwegian North Sea. *American Association of Petroleum Geologist,* **98**, 2019-2055.

MARSH, N., IMBER, J., HOLDSWORTH, R. E., BROCKBANK, P. & RINGROSE, P. 2010. The structural evolution of the Halten Terrace, offshore Mid-Norway: extensional fault growth and strain localisation in a multi-layer brittle–ductile system. *Basin Research*, **22**, 195-214.

MASSON, M. P. 1972. L'exploration pétrolière en Angola: *Revue de l'Association Française des Techniciens du Pétrole*, **212**, 21-34.

MCKIE, T. & WILLIAMS, B. 2009. Triassic palaeogeography and fluvial dispersal across the northwest Europe Basins. *Geological Journal*, **44**, 711–741.

MCLEOD, A. E., UNDERHILL, J., DAVIES, S. J. & DAWERS, N. H. 2002. The influence of fault array evolution on synrift sedimentation patterns: Controls on deposition in the Strathspey-Breny-Statfjord half graben, northern North Sea. *American Association of Petroleum Geologist,* **86**, 1061–1093.

MELLERE, D. & STEEL, R. J. 1996. Tidal sedimentation in Inner Hebrides half grabens, Scotland: the Mid-Jurassic Bearreraig Sandstone Formation. *Geological Society London,* Special Publication, **117**, 49–79.

828 NØTTVEDT, A., GABRIELSEN, R. H. & STEEL, R. J. 1995. Tectonostratigraphy and
829 sedimentary architecture of rift basins, with reference to the northern North Sea. *Marine*
830 *and Petroleum Geology*, **12**, 881-901.
831
832 PARTINGTON, M. A., COPESTAKE, P., MITCHENER, B. C. & UNDERHILL, J. R.
833 1993. Biostratigraphic calibration of genetic stratigraphic sequences in the Jurassic-
834 lowermost Cretaceous (Hettangian to Ryazanian) of the North Sea and adjacent areas. In:
835 PARKER, J. R. (ed.) *Petroleum Geology of Northwest Europe: Proceedings of the 4th*
836 *Conference.* The Geological Society of London, 371–386.
837
838 POPRAWSKI, C., BASILE, C., AGIRREZABALA, L.M., JAILLARD, E., GAUDIN, M.
839 & JACQUIN, T. 2014. Sedimentary and structural record of the Albian growth of the
840 Bakio diapir (the Basque Country, northern Spain). *Basin Research*, **26**, 746-766.
841
842 PROSSER, S. 1993. Rift-related linked depositional systems and their seismic expression.
843 In: WILLIAMS, G. D. & DOBB, A. (eds.) *Tectonics and Seismic Sequence Stratigraphy.*
844 *Geological Society London*, Special Publication, **71**, 35–66.
845
846 RATTEY, R. P. & HAYWARD, A. B. 1993. Sequence stratigraphy of a failed rift system:
847 the Middle Jurassic to Early Cretaceous basin evolution of the Central and Northern North
848 Sea. In: PARKER, J. R. (ed.) *Petroleum Geology of Northwest Europe: Proceedings of the*
849 *4th Conference*. Geological Society, London, 215–249.
850
851 RAVNÅS, R. & STEEL, R. J. 1998. Architecture of marine rift-basin successions.
852 *American Association of Petroleum Geologists*, Bulletin **82**, 110-146.

RAVNÅS, R., BONDEVIK, K., HELLAND-HANSEN, W., LOMO, L., RYSETH, A. & STEEL, R. J. 1997. Sedimentation history as an indicator of rift initiation and development: the Late Bajocian-Bathonian evolution of the Oseberg-Brage area, northern North Sea. *Norsk Geologisk Tidsskrift*, **77**, 205-232.

ROWAN G. 2014. Passive-margin salt basins: hyperextension, evaporate deposition, and, salt tectonics. *Basin Research*, **26**, 154-182.

SHELLEY, D.C. & LAWTON, T.F. 2005. Sequence stratigraphy of tidally influenced deposits in a salt-withdrawal minibasin:Upper sandstone member of the Potrerillos Formation (Paleocene), La Popa basin, northeastern Mexico. *American Association of Petroleum Geologists*, Bulletin **89**, 1157-1179.

SPATHOPOULOS, F., DOUBLEDAY, P. A. & HALLSWORTH, C. R. 2000. Structural and depositional controls on the distribution of the Upper Jurassic shallow marine sandstones in the Fife and Angus fields area, Quadrants 31 & 39, UK Central North Sea. *Marine and Petroleum Geology*, **17**, 1053-1082.

STEWART, S. A. 2007. Salt tectonics in the North Sea Basin: a structural style template for seismic interpreters. In: RIES, A. C., BUTLER, R.W.H. & GRAHAM, R.H. (eds.) *Deformation of the Continental Crust: The Legacy of Mike Coward.* The Geological Society of London, Special Publication 272, 361–396.

STEWART, S. A. & CLARK, J. A. 1999. Impact of salt on the structure of the Central North Sea hydrocarbon fairways. In: FLEET, J. & BOLDY, S. A. R. (eds.) *Petroleum Geology of Northwest Europe: Proceedings of the 5th Conference*. The Geological Society of London, 179–200.

STEWART, S. A., HARVEY, M. J., OTTO, S. C. & WESTON, P. J. 1996. Influence of salt on fault geometry: examples from UK salt basins. The Geological Society of London, Special Publications **100**, 175-202. doi: 10.1144/GSL.SP.1996.100.01.12

UNDERHILL, J. & PARTINGTON, M. A. 1993. Jurassic thermal doming and deflation in the North Sea: implications of the sequence stratigraphic evidence. In: PARKER, J. R., (ed.) *Petroleum Geology of Northwest Europe: Proceedings of the 4th Conference*. The Geological Society of London, 337-345.

VENDEVILLE, B. C. & JACKSON, M. P. A. 1992a. The rise of diapirs during thin-skinned extension. *Marine and Petroleum Geology*, **9**, 331–353.

VOLLSET, J. & DORÉ, A.G. 1984. A revised Triassic and Jurassic lithostratigraphic nomenclature for the Norwegian North Sea. *Norwegian Petroleum Society*. Bulletin **3**.

WAKEFIELD, L. L., DROSTE, H., GILES, M. R. & JANSSEN, R. 1993. Late Jurassic plays along the western margin of the Central Graben. In: PARKER, J. R. (ed.) *Petroleum Geology of Northwest Europe: Proceedings of the 4th Conference*. The Geological Society of London, 459-468.

WILSON, P., ELLIOTT, G. M., GAWTHORPE, R. L., JACKSON, C. A. L., MICHELSEN, L. & SHARP, I. R. 2013. Geometry and segmentation of an evaporite-detached normal fault array: 3D seismic analysis of the southern Bremstein Fault Complex, offshore mid-Norway. *Journal of Structural Geology*, **51**, 74-91.

ZANELLA, E. & COWARD, M.P. 2003. Structural framework. In: Evans D., Graham C., Armour A. & Bathurst P. (eds.), The Millennium Atlas: Petroleum Geology of the Central and Northern North Sea. The Geological Society of London, 45-59.

FIGURE CAPTIONS

Fig. 1: Regional geographic setting of the North Sea trilete rift system, showing the limit of the Zechstein Supergroup in the North Permian Basin (taken from Zanella & Coward 2003).
(VG: Viking Graben; MF: Moray Firth; CG: Central Graben: O-B: Oseberg-Brage; T-E: Tern-Eider horst; N-H-D: Ninian-Hutton-Dunlin fault system; A-B-S: North Alwyn-Brent-Statfjord fault system)

Fig. 2: Regional tectono-stratigraphic chart for areas between the Cod Terrace and the Norwegian-Danish Basin, on the eastern flank of the Central Graben (labelled as study area in Fig. 1) (modified from Vollset & Doré 1984), showing major flooding surfaces documented in regional literature (Partington et al. 1993), age dates (International Stratigraphic Chart 2014), main tectonic events, and surfaces interpreted in seismic, well-log and core data from the study area.

Fig. 3: SW-NE chronostratigraphic cross-section illustrating diachronous deposition

927 of net-transgressive Upper Jurassic strata in the Central North Sea (modified from
928 Partington et al. 1993 and Hampson et al. 2009). See Figure 1 for location of cross-section.
929
930 Fig. 4: Simplified structure map illustrating major present day topographic features in the
931 study area, and the distribution of seismic and well data used for this study. (SH: Sele
932 High; EB: Egersund Basin; LN: Lista Nose; N-DB: Norwegian-Danish Basin; SVH:
933 Sørvestlandet High; CT: Cod Terrace; CG: Central Graben; SP: Stavanger Platform)
934
935 Fig. 5: Interpreted SW-NE regional line of section from the Cod Terrace to the Stavanger
936 Platform illustrating the presence and distribution of sub-salt normal faults, salt structures,
937 and supra-salt normal faults. (b) Cosine of instantaneous phase section from the Cod
938 Terrace showing detailed mapping and onlap of Jurassic reflectors on to the margins of
939 minibasins developed above salt walls (located on Fig. 5d). (c) Cosine of instantaneous
940 phase section from the Egersund Basin showing laterally continuous Upper Jurassic
941 reflectors that record gradual lateral thinning from the flank to the crest of salt structures
942 (located on Fig. 5e). (d) Isochron map between the J66FS-near Top Jurassic (K10FS)
943 flooding surfaces on the Cod Terrace showing stratigraphic thickness variations across
944 supra-salt normal faults (Figs 4 and 5b). (e) Isochron map between the near top Jurassic-
945 Top Triassic surfaces showing thickness changes between supra-salt grabens in the
946 Egersund Basin (Figs 4 and 5c).
947
948 Fig. 6: Two-way time (TWT) maps for: (a) top Rotliegend structure, illustrating sub-salt,
949 basement structures; (b) top Zechstein isochron, illustrating various types of salt structures,
950 including salt walls, salt rollers, and salt welds; (c) top Mandal structure, illustrating supra-

951 salt, cover structures on the Cod Terrace (located on Fig. 6b); and (d) top Egersund
952 illustrating supra-salt cover structures in the Egersund Basin
953 (located on Fig. 6b). (SH: Sele High; EB: Egersund Basin; LN: Lista Nose; N-DB:
954 Norwegian-Danish Basin; SVH: Sørvestlandet High; CT: Cod Terrace; CG: Central
955 Graben; SP: Stavanger Platform)
956
957 Fig. 7: (a) SW-NE wireline-log correlation panel and (b) corresponding
958 chronostratigraphic cross-section across the Cod Terrace, Sørvestlandet High, Norwegian-
959 Danish Basin, Egersund Basin, and Stavanger Platform illustrating the temporal and
960 spatial variation of Middle-to-Upper Jurassic net-transgressive strata of the Norwegian
961 Central Graben. See Figure 4 for location.
962
963 Fig. 8: (a) NW-SE wireline-log correlation panel and (b) corresponding
964 chronostratigraphic cross-section across the Egersund Basin, illustrating the temporal and
965 spatial variation of Middle-to-Upper Jurassic net-transgressive strata of the Norwegian
966 Central Graben. See Figure 4 for location and Figure 7 for legend.
967
968 Fig. 9: Series of palaeogeographic maps that illustrate the tectono-stratigraphic evolution
969 of the Middle-to-Upper Jurassic succession in the Norwegian North Sea: (a) Late
970 Callovian (below FS2); (b) Late Oxfordian (below J56FS); (c) Early Kimmeridgian
971 (below J62FS); (d) Late Kimmeridgian (below J66AFS); (e) Portlandian (below J71FS);
972 and (f) Late Ryazanian (below K10FS). (SH: Sele High; EB: Egersund Basin; LN: Lista
973 Nose; N-DB: Norwegian-Danish Basin; SVH: Sørvestlandet High; CT: Cod Terrace; SP:
974 Stavanger Platform)
975

976 Fig. 10: Schematic block diagrams illustrating structural styles and coastal-plain-to-marine
977 depositional environments for: (a) a generic, salt-free rift basin (taken from Gawthorpe and
978 Leeder, 2000); (b) the salt-influenced Norwegian Central North Sea rift basin.
979
980 **TABLE CAPTIONS**
981
982 Table 1: Summary of facies association in the Upper Jurassic Ula, Gyda and Sandnes
983 formations (Mannie et al. 2014a, b).
984
985 Table 2: Summary of the thickness and facies variations for the various sub-, intra- and
986 supra-salt structural styles in the study area (Mannie et al. 2014a, b). See Figure 5 for
987 structural styles identified
988

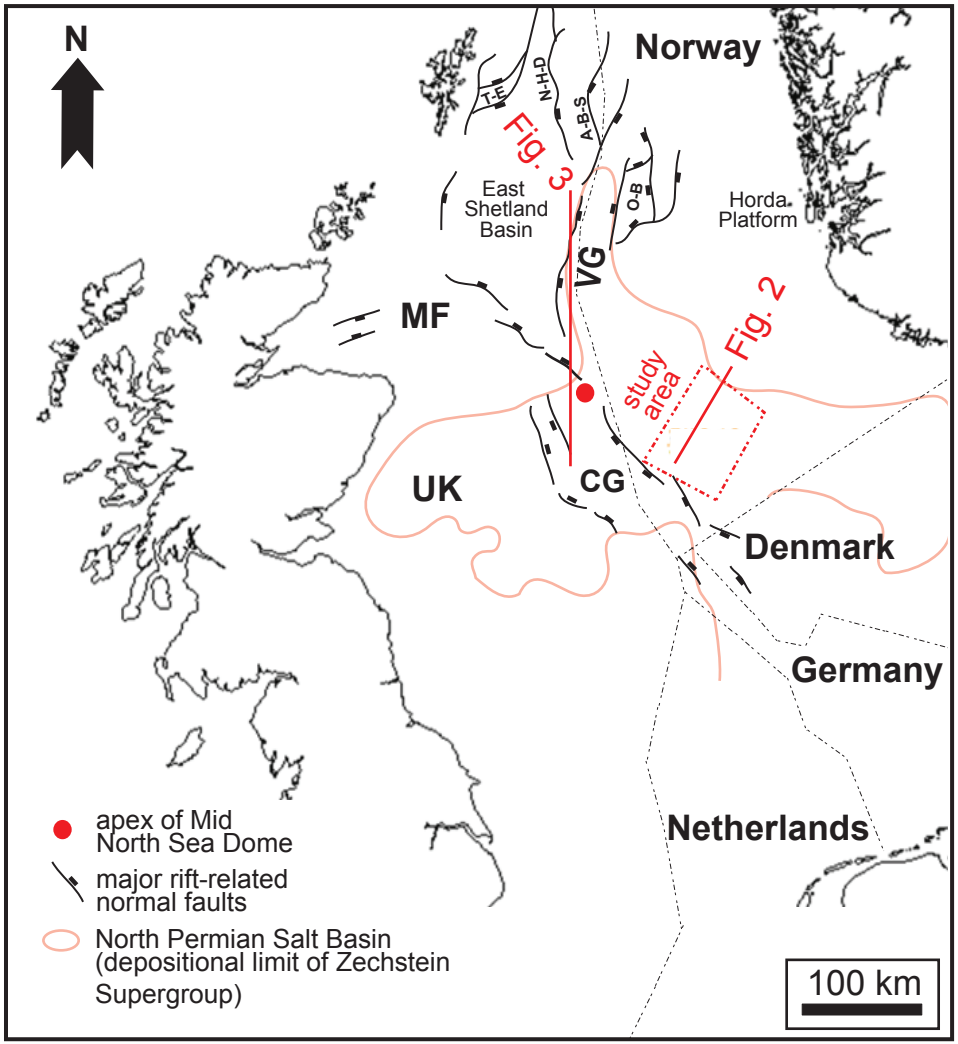

Fig. 1: Regional geographic setting of the North Sea trilete rift system, showing the limit of the Zechstein Supergroup in the North Permian Basin (taken from Smith et al. 1993). (VG: Viking Graben; MF: Moray Firth; CG: Central Graben; O-B:Oseberg-Brage; T-E: Tern-Eider horst; N-H-D: Ninian-Hutton-Dunlin fault system; A-B-S: North Alwyn-Brent-Statfjord fault system)

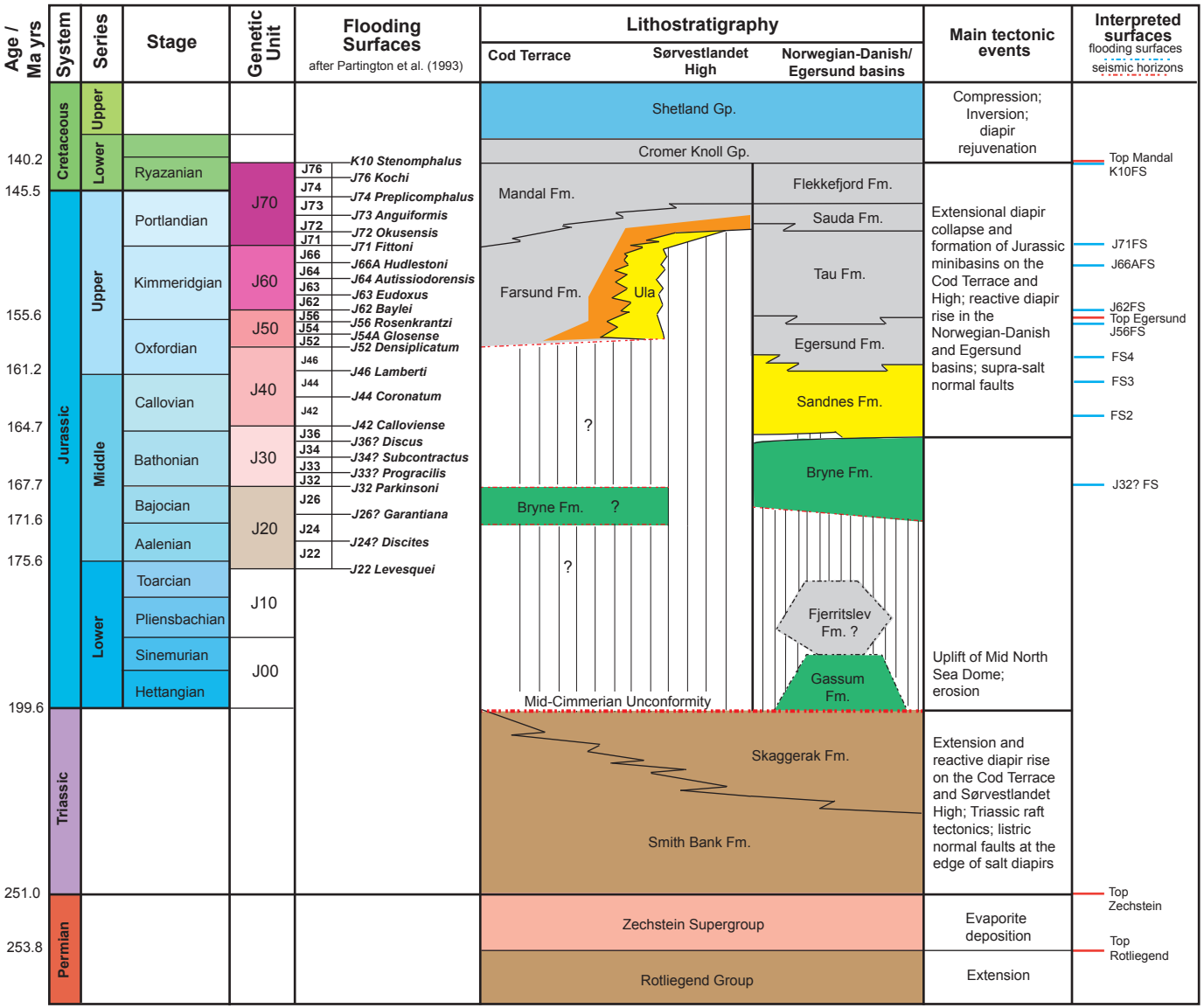

Fig. 2: Regional tectono-stratigraphic chart for areas between the Cod Terrace and the Norwegian-Danish Basin, on the eastern flank of the Central Graben (labelled as study area in Fig. 1) (modified from Vollset & Doré 1984), showing major flooding surfaces documented in regional literature (Partington et al. 1993), age dates (International Stratigraphic Chart 2014), main tectonic events, and surfaces interpreted in seismic, well-log and core data from the

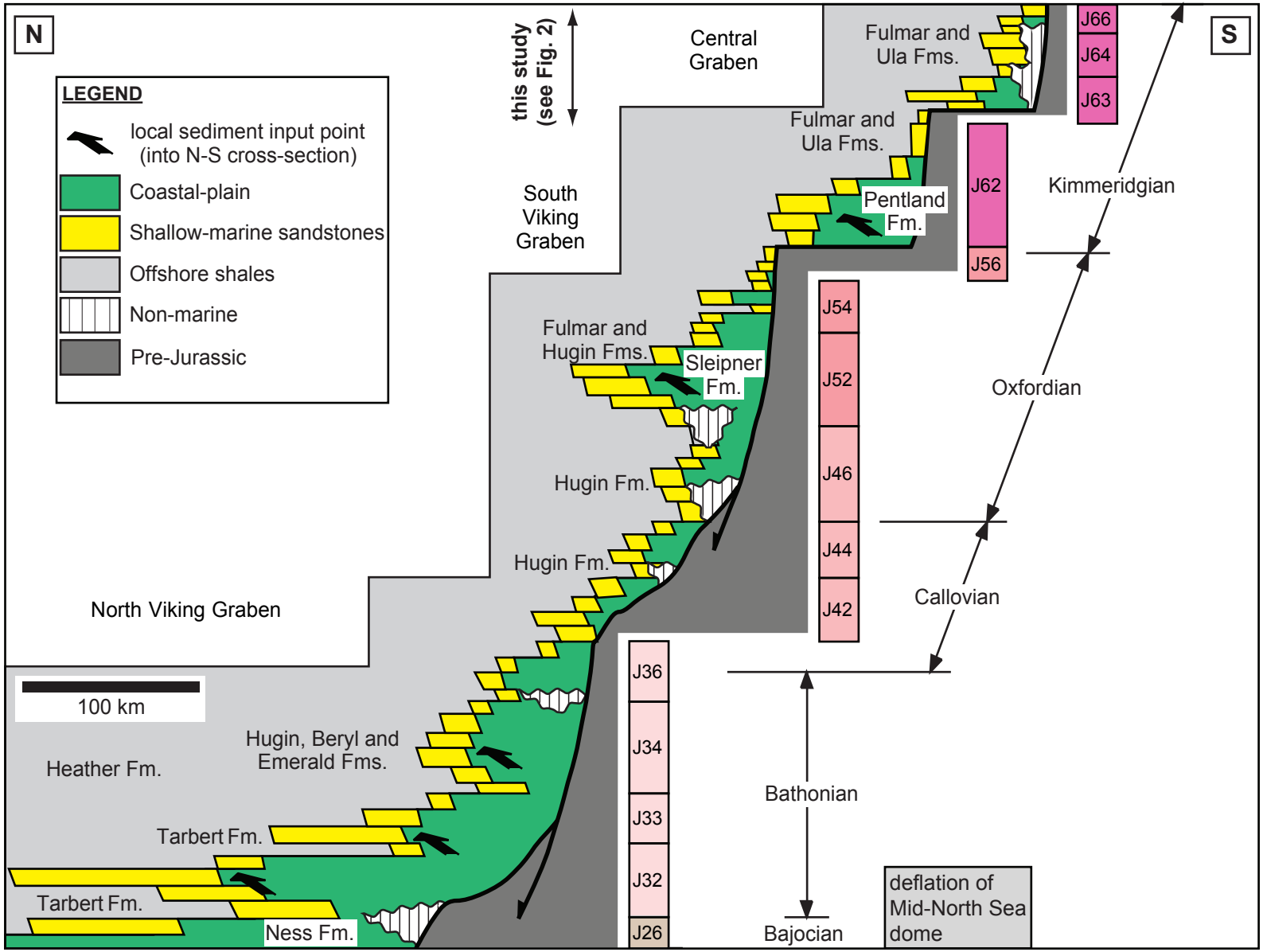
N
S
LEGEND
local sediment input point (into N-S cross-section)
Coastal-plain
Shallow-marine sandstones
Offshore shales
Non-marine
Pre-Jurassic
this study (see Fig. 2)
Central Graben
South Viking Graben
North Viking Graben
Fulmar and Ula Fms.
Fulmar and Ula Fms.
Pentland Fm.
Fulmar and Hugin Fms.
Sleipner Fm.
Hugin Fm.
Hugin Fm.
Hugin, Beryl and Emerald Fms.
Heather Fm.
Tarbert Fm.
Tarbert Fm.
Ness Fm.
100 km
J66
J64
J63
J62
J56
J54
J52
J46
J44
J42
J36
J34
J33
J32
J26
Kimmeridgian
Oxfordian
Callovian
Bathonian
Bajocian
deflation of Mid-North Sea dome

Fig. 3

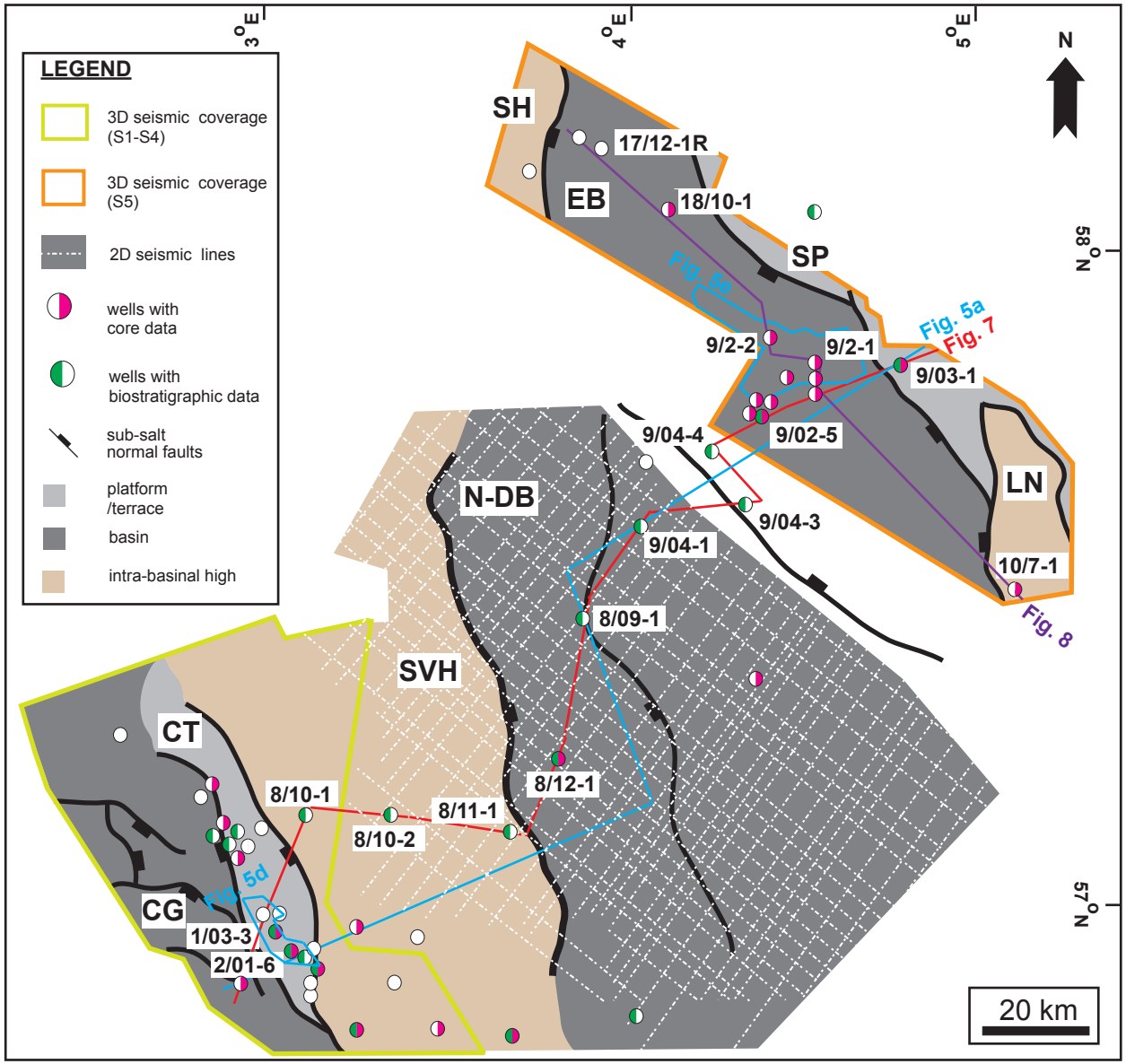

Fig. 4: Simplified structure map illustrating major present day topographic features in the study area, and the distribution of seismic and well data used for this study. (SH: Sele High; EB: Egersund Basin; LN: Lista Nose; N-DB: Norwegian-Danish Basin; SVH: Sørvestlandet High; CT: Cod Terrace; CG: Central Graben; SP: Stavanger Platform)

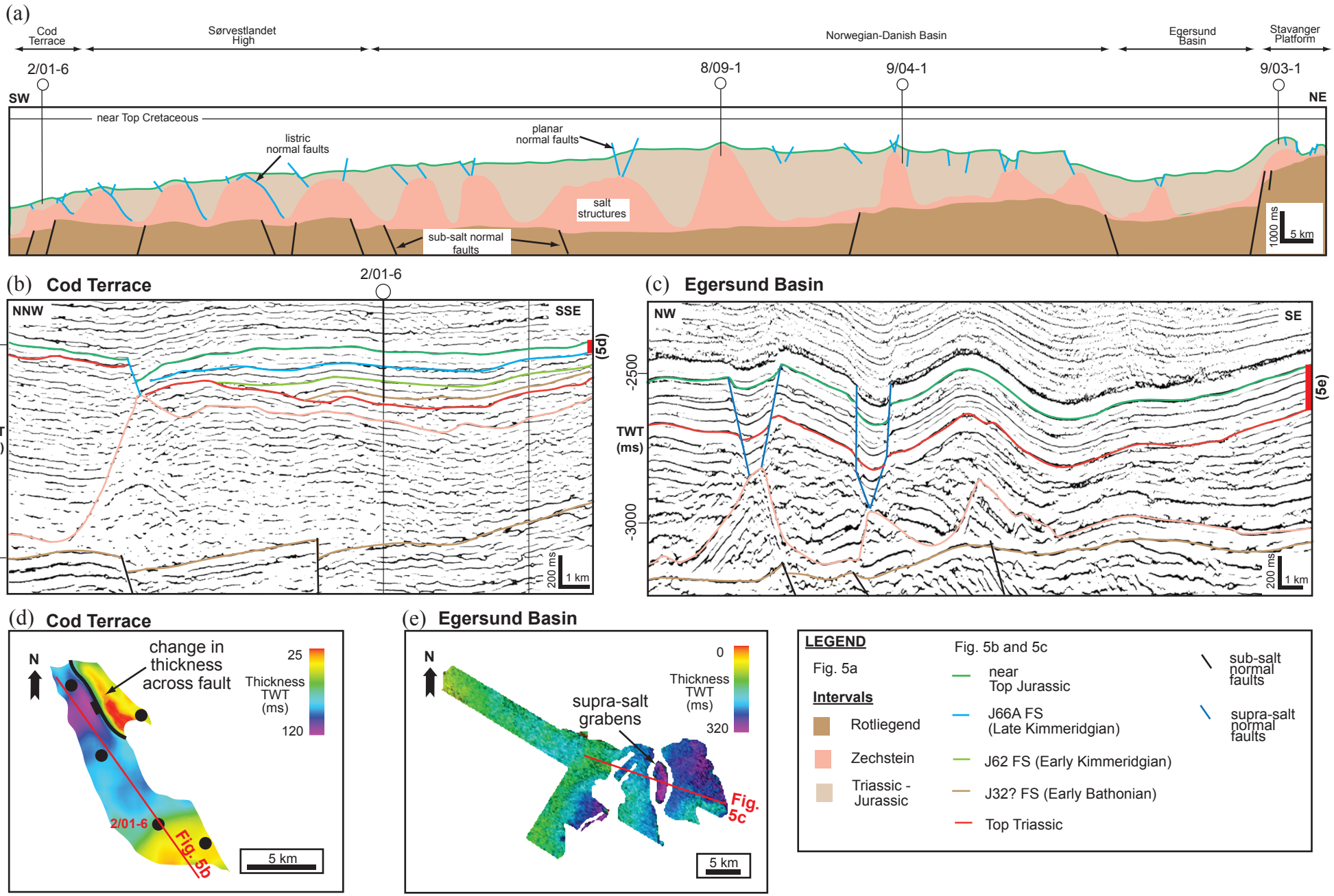
(a)
Cod Terrace
Sørvestlandet High
Norwegian-Danish Basin
Egersund Basin
Stavanger Platform
2/01-6
8/09-1
9/04-1
9/03-1
SW
NE
near Top Cretaceous
listric normal faults
planar normal faults
salt structures
sub-salt normal faults
1000 ms
5 km
(b) Cod Terrace
2/01-6
NNW
SSE
(5d)
-3500
-4500
TWT (ms)
200 ms
1 km
(c) Egersund Basin
NW
SE
(5e)
-2500
-3000
TWT (ms)
200 ms
1 km
(d) Cod Terrace
N
change in thickness across fault
25
Thickness TWT (ms)
120
2/01-6
Fig. 5b
5 km
(e) Egersund Basin
N
0
Thickness TWT (ms)
320
supra-salt grabens
Fig. 5c
5 km
LEGEND
Fig. 5a
Intervals
Rotliegend
Zechstein
Triassic - Jurassic
Fig. 5b and 5c
near Top Jurassic
J66A FS (Late Kimmeridgian)
J62 FS (Early Kimmeridgian)
J32? FS (Early Bathonian)
Top Triassic
sub-salt normal faults
supra-salt normal faults

Fig. 5: Interpreted SW-NE regional line of section from the Cod Terrace to the Stavanger Platform illustrating the presence and distribution of sub-salt normal faults, salt structures, and supra-salt normal faults. (b) Cosine of instantaneous phase section from the Cod Terrace showing detailed mapping and onlap of Jurassic reflectors on to the margins of minibasins developed above salt walls (located on Fig. 5d). (c) Cosine of instantaneous phase section from the Egersund Basin showing laterally continuous Upper Jurassic reflectors that record gradual lateral thinning from the flank to the crest of salt structures (located on Fig. 5e). (d) Isochron map between the J66FS-near Top Jurassic flooding surfaces on the Cod Terrace showing stratigraphic thickness variations across supra-salt normal faults (Figs 4 and 5b). (e) Isochron map between the near top Jurassic-Top Triassic surfaces showing thickness changes between supra-salt grabens in the Egersund Basin (Figs 4 and 5c).

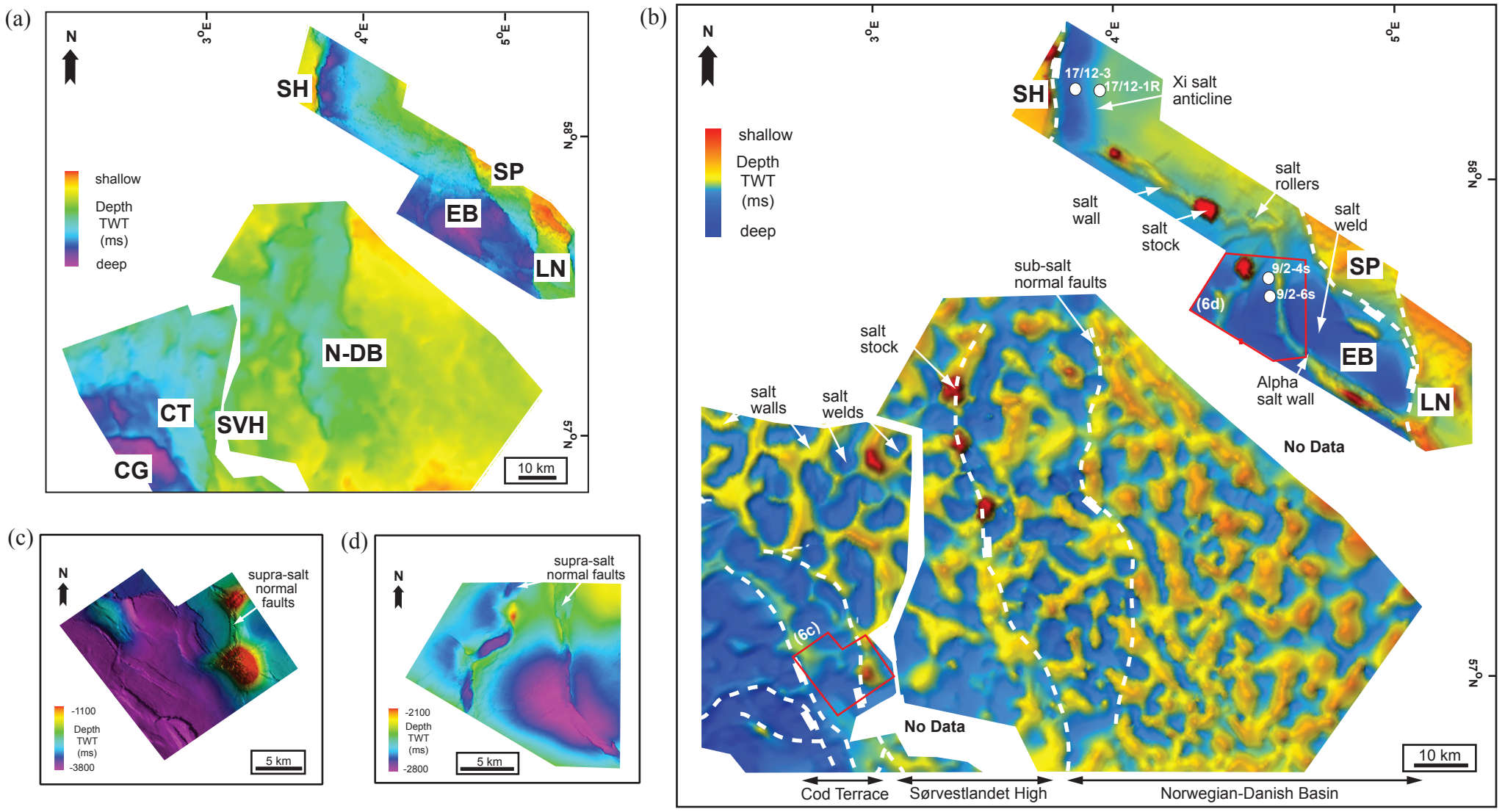

Fig. 6: Two-way time (TWT) maps for: (a) top Rotliegend structure, illustrating sub-salt, basement structures; (b) top Zechstein isochron, illustrating various types of salt structures, including salt walls, salt diapirs, salt rollers, salt pillows and salt welds; (c) top Mandal structure, illustrating supra-salt, cover structures on the Cod Terrace (located on Fig. 6b); and (d) top Egersund structure illustrating supra-salt cover structures in the Egersund Basin (located on Fig. 6b). (SH: Sele High; EB: Egersund Basin; LN: Lista Nose; N-DB: Norwegian-Danish Basin; SVH: Sørvestlandet High; CT: Cod Terrace; CG: Central Graben; SP: Stavanger Platform)

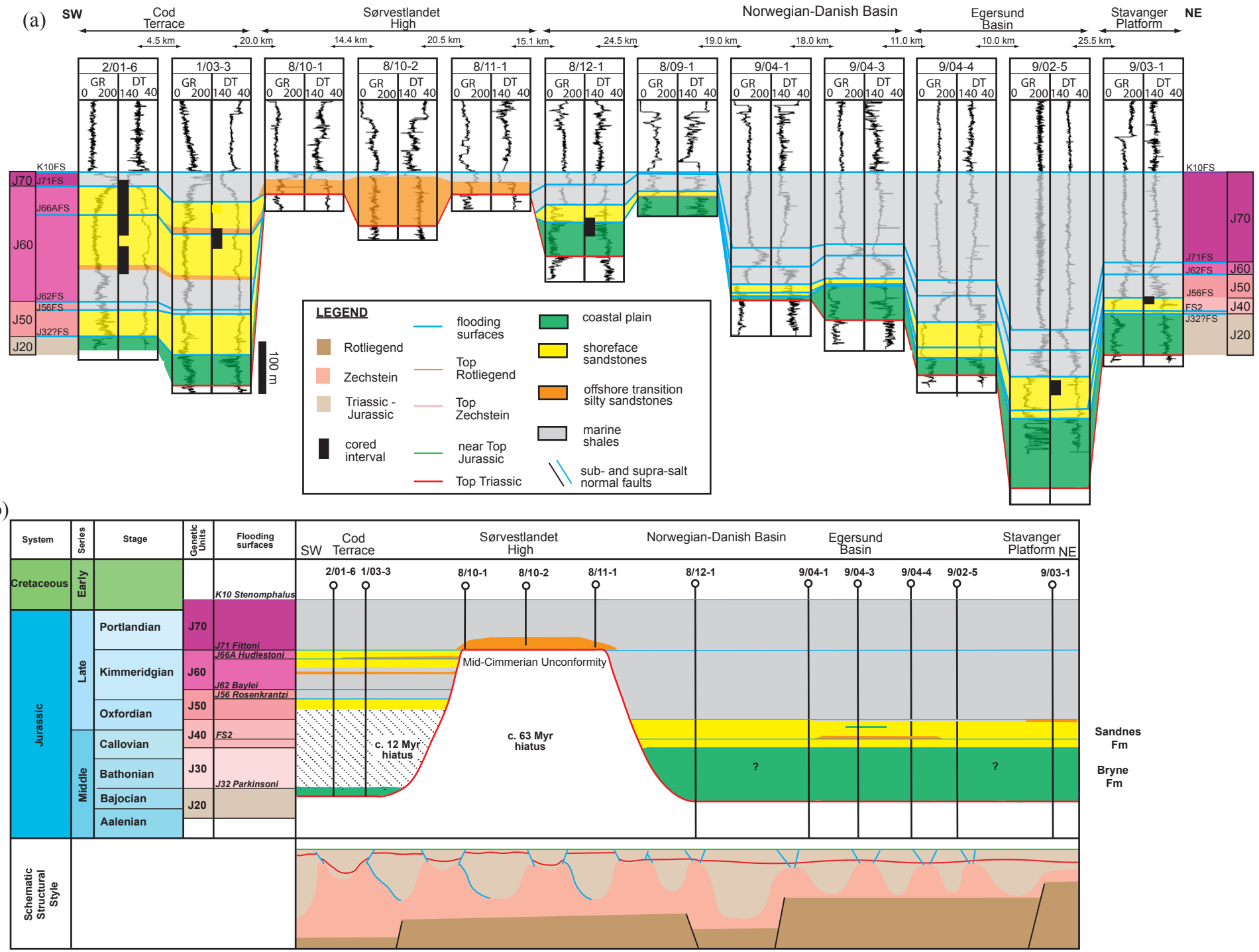
(a)
SW
NE
Cod Terrace
Sørvestlandet High
Norwegian-Danish Basin
Egersund Basin
Stavanger Platform
4.5 km
20.0 km
14.4 km
20.5 km
15.1 km
24.5 km
19.0 km
18.0 km
11.0 km
10.0 km
25.5 km
2/01-6
1/03-3
8/10-1
8/10-2
8/11-1
8/12-1
8/09-1
9/04-1
9/04-3
9/04-4
9/02-5
9/03-1
GR 0 200
DT 140 40
K10FS
J70
J71FS
J66AFS
J60
J62FS
J56FS
J50
J32?FS
J20
J62FS
J56FS
FS2
J32?FS
J70
J60
J50
J40
J20
100 m
LEGEND
Rotliegend
Zechstein
Triassic - Jurassic
cored interval
flooding surfaces
Top Rotliegend
Top Zechstein
near Top Jurassic
Top Triassic
coastal plain
shoreface sandstones
offshore transition silty sandstones
marine shales
sub- and supra-salt normal faults
(b)
System
Series
Stage
Genetic Units
Flooding surfaces
Cretaceous
Early
K10 Stenomphalus
Jurassic
Late
Middle
Portlandian
Kimmeridgian
Oxfordian
Callovian
Bathonian
Bajocian
Aalenian
J70
J60
J50
J40
J30
J20
J71 Fittoni
J66A Hudlestoni
J62 Baylei
J56 Rosenkrantzi
FS2
J32 Parkinsoni
Schematic Structural Style
SW
Cod Terrace
Sørvestlandet High
Norwegian-Danish Basin
Egersund Basin
Stavanger Platform
NE
2/01-6
1/03-3
8/10-1
8/10-2
8/11-1
8/12-1
9/04-1
9/04-3
9/04-4
9/02-5
9/03-1
Mid-Cimmerian Unconformity
c. 12 Myr hiatus
c. 63 Myr hiatus
?
?
Sandnes Fm
Bryne Fm

Fig. 7:(a) SW-NE wireline-log correlation panel and (b) corresponding chronostratigraphic cross-section across the Cod Terrace, Sørvestlandet High, Norwegian-Danish Basin, Egersund Basin, and Stavanger Platform illustrating the temporal and spatial variation of Middle-to-Upper Jurassic net-transgressive strata of the Norwegian Central Graben. See Figure 4 for location.

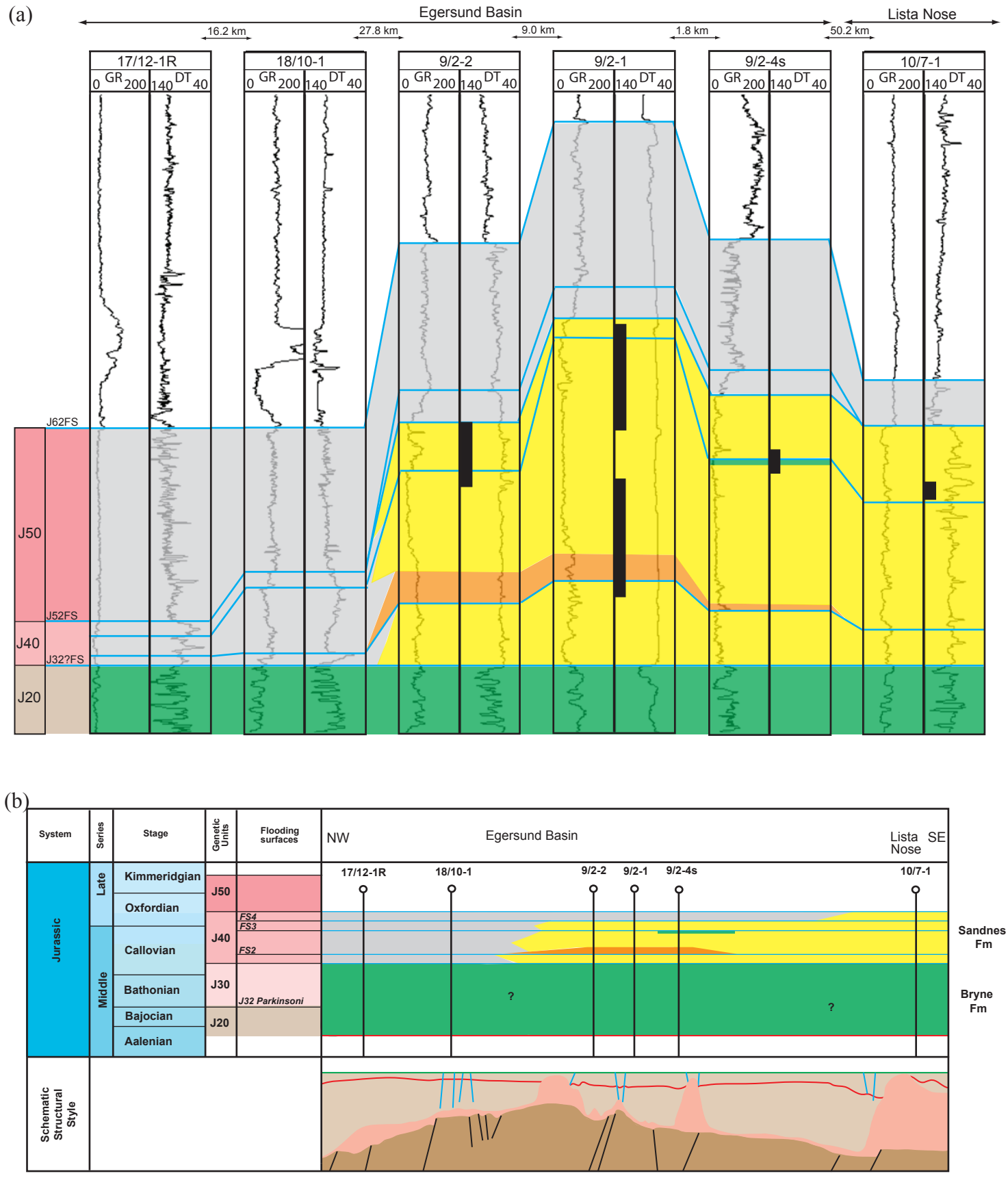

Fig. 8:(a) NW-SE wireline-log correlation panel and (b) corresponding chronostratigraphic cross-section across the Egersund Basin, illustrating the temporal and spatial variation of Middle-to-Upper Jurassic net-transgressive strata of the Norwegian Central Graben. See Figure 4 for location.

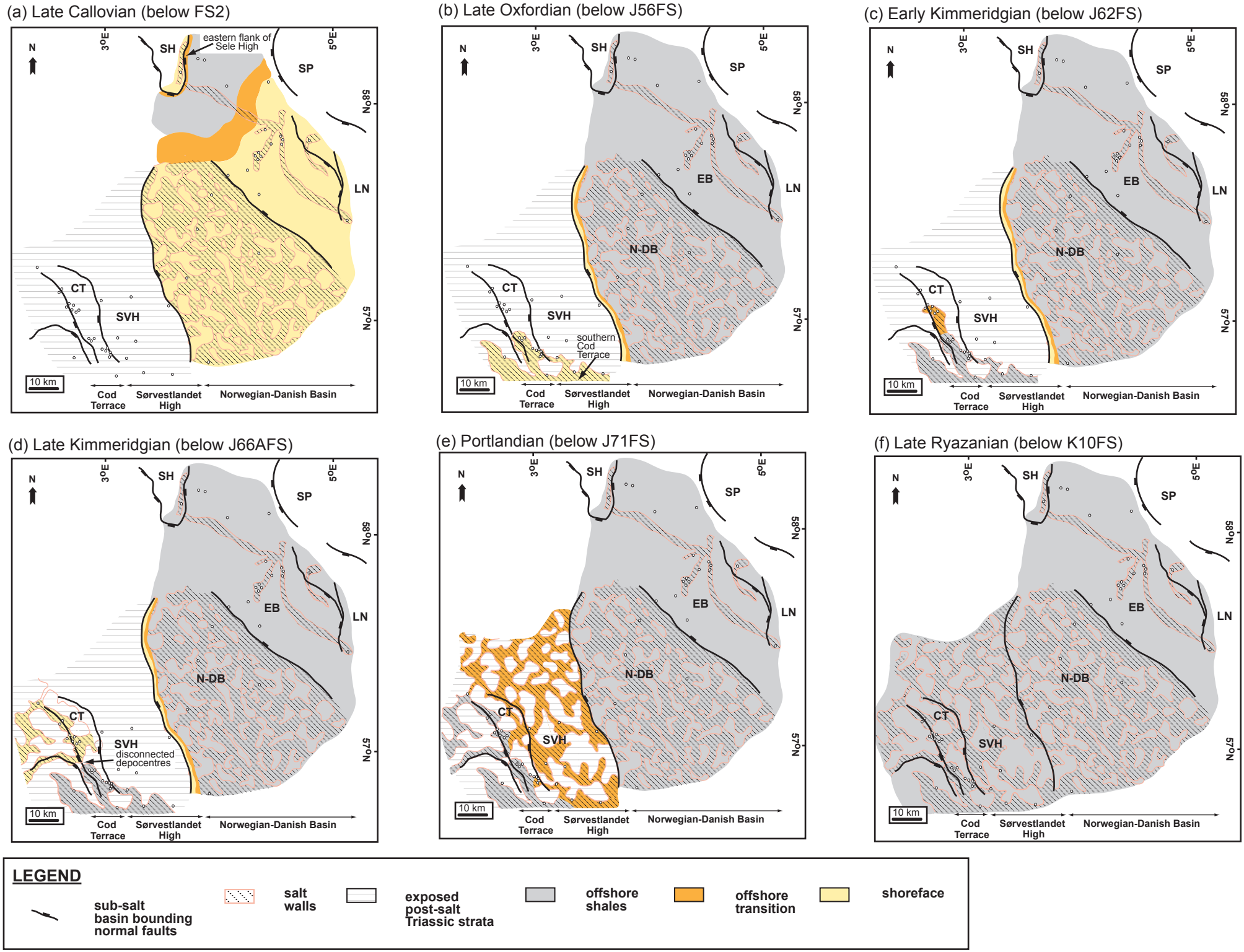
(a) Late Callovian (below FS2)
(b) Late Oxfordian (below J56FS)
(c) Early Kimmeridgian (below J62FS)
(d) Late Kimmeridgian (below J66AFS)
(e) Portlandian (below J71FS)
(f) Late Ryazanian (below K10FS)
N
3°E
5°E
58°N
57°N
SH
SP
LN
EB
N-DB
CT
SVH
eastern flank of Sele High
southern Cod Terrace
disconnected depocentres
10 km
Cod Terrace
Sørvestlandet High
Norwegian-Danish Basin
LEGEND
sub-salt basin bounding normal faults
salt walls
exposed post-salt Triassic strata
offshore shales
offshore transition
shoreface

Fig. 9: Series of palaeogeographic maps that illustrate the tectono-stratigraphic evolution of the Middle-to-Upper Jurassic succession in the Norwegian North Sea: (a) Late Callovian (below FS2); (b) Late Oxfordian (below J56FS); (c) Early Kimmeridgian (below J62FS); (d) Late Kimmeridgian (below J66AFS); (e) Portlandian (below J71FS); and (f) Late Ryazanian (below K10FS). (SH: Sele High; EB: Egersund Basin; LN: Lista Nose; N-DB: Norwegian-Danish Basin; SVH: Sørvestlandet High; CT: Cod Terrace; SP: Stavanger Platform)

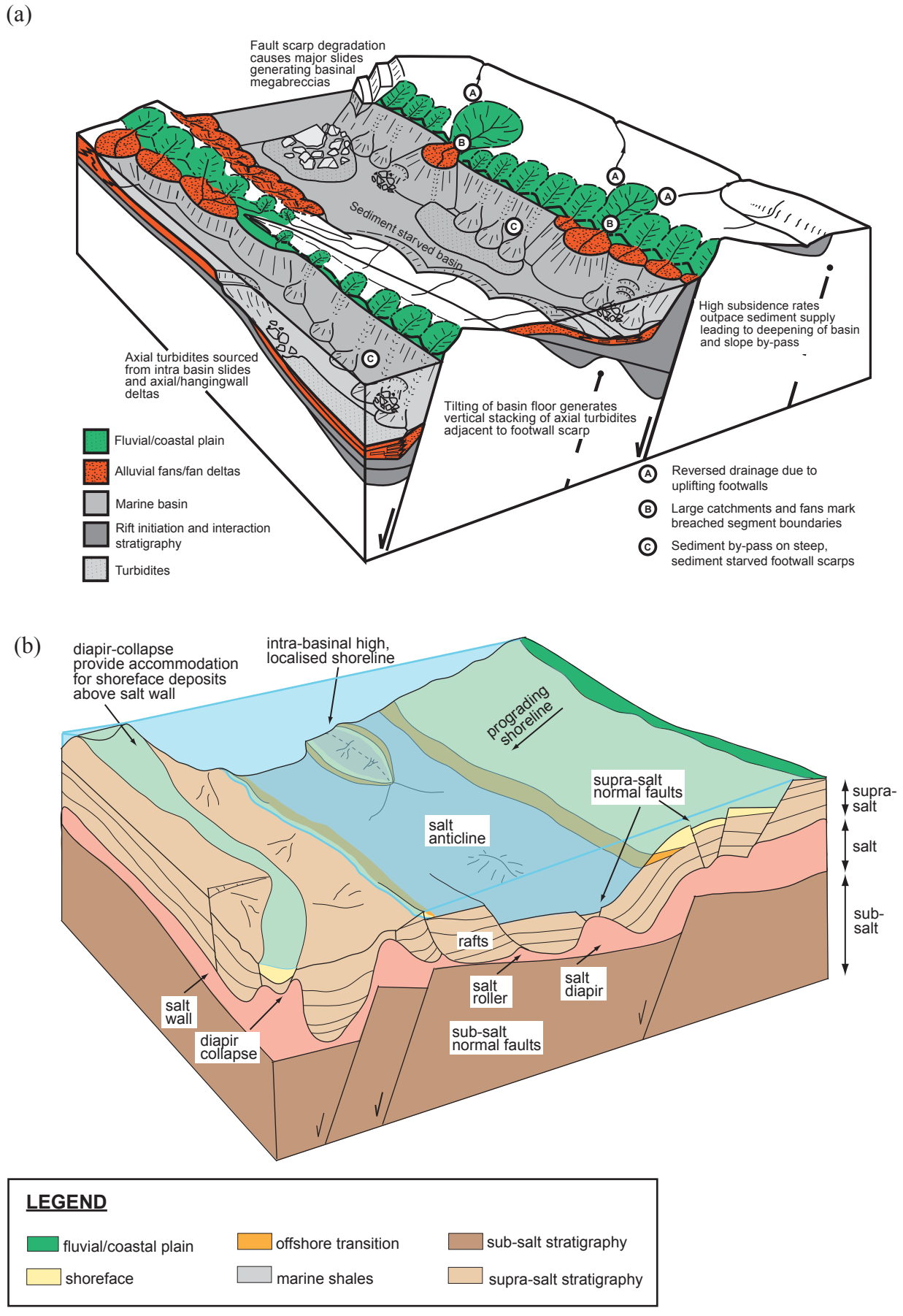

Fig. 10: Schematic block diagrams illustrating structural styles and coastal-plain-to-marine depositional environments for: (a) a generic, salt-free rift basin (taken from Gawthorpe and Leeder, 2000); (b) the salt-influenced Norwegian Central North Sea rift basin.